


Review

Metallogenic Evolution Related to Mantle Delamination Under Northern Tunisia

Nejib Jemmali ^{1,2,*} , Fouad Souissi ^{2,3}, Larbi Rddad ⁴ , Emmanuel John Carranza ⁵  and Guillermo Booth-Rea ⁶ 

¹ Faculty of Sciences of Gafsa, Department of Geology, University of Gafsa, Sidi Ahmed Zarrouk, Gafsa 2112, Tunisia

² Laboratory of Useful Materials, National Institute of Research and Physicochemical Analysis, Technopole Sidi Thabet, Ariana 2026, Tunisia; souissifoued2@gmail.com

³ Faculty of Sciences of Tunis, University of Tunis El Manar, Tunis 2092, Tunisia

⁴ Earth and Planetary Science Division, Department of Physical Sciences, Kingsborough Community College, City University of New York, 2001 Oriental Boulevard, Brooklyn, New York, NY 11235-2398, USA; lrddad@gmail.com

⁵ Discipline of Geological Sciences, School of Agricultural, Earth and Environmental Sciences, University of KwaZulu-Natal, Westville Campus, Durban 4041, South Africa; ejmccarranza@gmail.com

⁶ Department of Geodynamics, University of Granada, 18071 Granada, Spain; gbooth@go.ugr.es

* Correspondence: nejib.jemmali@yahoo.fr or jemmali.nejib@gmail.com

Abstract: Mineralization processes in the Tell-Atlas of North Africa coincided with magmatism, extension, and lithospheric rejuvenation during the middle to late Miocene. This review examines the lead isotope compositions and Pb-Pb age dating of ore deposits in the region to elucidate the sources and timing of mineralization events. The data reveal a predominantly radiogenic signature in the ores, indicating that the primary component is from a crustal source, with a contribution from the mantle. Pb-Pb age dating suggests the ranges of mineralization ages, with late Miocene events being particularly significant, coinciding with proposed sub-continental mantle delamination following subduction of the African lithosphere. In this context, polymetallic mineralizations formed related to felsic magmatism, hydrothermalism driven by extensional faults, resulting in the formation of Mississippi Valley-Type, and Sedimentary exhalative deposits within associated semi-grabens and diapirism. The correlation between orogenic extensional collapse, magmatism, and mineralization underscores the importance of understanding the specific geological context of ore formation. The detachment of subducted slabs and subsequent influx of hot asthenosphere play pivotal roles in creating conducive conditions for mineralization. This study sheds light on the intricate interplay between tectonic mechanisms, mantle-crust interactions, and mineralization events in the Tell-Atlas, offering insights for further exploration in the region.

Keywords: mineralization; Atlas Mountains; lead isotopes; orogenic collapse; lithospheric delamination; asthenosphere; Miocene; Tunisia



Academic Editor: Xiaoyong Yang

Received: 19 November 2024

Revised: 16 December 2024

Accepted: 25 December 2024

Published: 30 December 2024

Citation: Jemmali, N.; Souissi, F.; Rddad, L.; Carranza, E.J.; Booth-Rea, G. Metallogenic Evolution Related to Mantle Delamination Under Northern Tunisia. *Minerals* **2025**, *15*, 31. <https://doi.org/10.3390/min15010031>

Copyright: © 2024 by the authors. Licensee MDPI, Basel, Switzerland. This article is an open access article distributed under the terms and conditions of the Creative Commons Attribution (CC BY) license (<https://creativecommons.org/licenses/by/4.0/>).

1. Introduction

Subcontinental mantle delamination and/or detachment has driven the upwelling of hot asthenosphere under extending orogenic domains during the Neogene evolution of the Western Mediterranean (e.g., [1–11]). The delamination and slab detachment mechanisms renew the lithosphere, enhancing heat and fluid circulation within the thinned delaminated regions, and hence favoring a diverse range of mineralization, often related to magmatism [2,12]. Furthermore, mineralizing fluids are driven through fault systems deeply

rooted in the Earth's crust, with a connection to the mantle that facilitates the circulation of magmatic and crustal fluids containing metals [13–17]. These tectonic processes migrate following retreating mantle slabs, producing various mineralizing mechanisms. These processes include mantle flow and fertilization, lower-crustal melting, magmatism, the extensional exhumation of metamorphic domes, hydrothermalism, topographic uplift, and the formation of sedimentary basins [3,8–10,18,19].

Here, we review the role of mantle delamination or detachment in the formation of the great diversity of ore deposits in the Nappes zone. Ore deposits within the Tellian domain (Nappes zone) in Northern Tunisia are commonly attributed to structures formed during the Tell orogenic evolution, such as strike-slip faulting, thrusting, or diapirism. These mineralizations include the Oued Belif iron oxide-uranium (gold) deposit, which is related to Iron Oxide Copper Gold-type deposits (IOCG-type) [20], SEDEX Pb-Zn deposits of Sidi Driss and Douahria semi grabens [21], and Cu-rich sulfides of Ain El Bey and Chouichia [22], as well as Mississippi Valley Type Pb-Zn-(Ba-Sr) deposits, Jebel Ghozlane, and Ain Allega [23–25]. However, recent works have identified an extensional tectonic setting coeval to Si-K rich and basaltic alkaline magmatism for the late Miocene evolution of the region [9,10], leading to the reinterpretation for the genesis of some mineralization within this context [15,16].

In the current review, we re-evaluate the origin and evolution of late Miocene mineralizations in Northern Tunisia, categorizing them according to the different settings identified in the recently established extensional and lithospheric rejuvenation context. To achieve this objective, we reviewed previously published lead isotope data from various ore deposits within the Nappes zone, including MVT (e.g., Jalta, Jebel Ghozlane, Fedj Hassene, and Jebel Hallouf [23,24,26,27]), SEDEX (e.g., Sidi Driss and Douahria [21]), mixed type (e.g., Oued Maden [27]), and IOGC (e.g., Oued Belif hematite-rich breccia [20,28]). Additionally, we have acquired new lead isotope geochemistry for Ain Allega. We compare these Pb isotope datasets from ore deposits within the Nappes zone to shed light on the sources of Pb and the timing of ore mineralization. This comparison extends to those in Northern Africa (Algeria and Morocco) and southeastern Spain, highlighting a possible relationship between mineralization and Miocene extensional structures, as well as magmatism resulting from mantle lithospheric delamination.

2. Regional Geology

The Maghrebian orogenic belt comprises two different domains: (i) the Alboran-Kabylias-Peloritan-Calabria (AlKaPeCa; [29]) and (ii) the Tell-Rif external zone to the north and the inverted Atlas belt to the south ([30]; Figure 1). The Alboran-Kabylias-Peloritan-Calabria (AlKaPeCa; [29]) hinterland domain is of European origin and represents the former northern margin of the Alpine Tethys [29,31–34]. The Tell-Rif Western Mediterranean Alpine belts result from the closure of the Maghrebian branch of the Alpine Tethys (Figure 1). The Atlas, belonging to the second domain, is an intra-continental asymmetric system that includes both poorly deformed mountain belts (High and Middle Atlas in Morocco, the Saharan Atlas and Aurès Mountains in Algeria, and the Tunisian Atlas in Tunisia). This system is characterized by the widespread distribution of older rocks (Paleozoic and lower Mesozoic) in the western Maghreb and Cenozoic rocks that dominate in the eastern part ([30,32]; Figure 1).

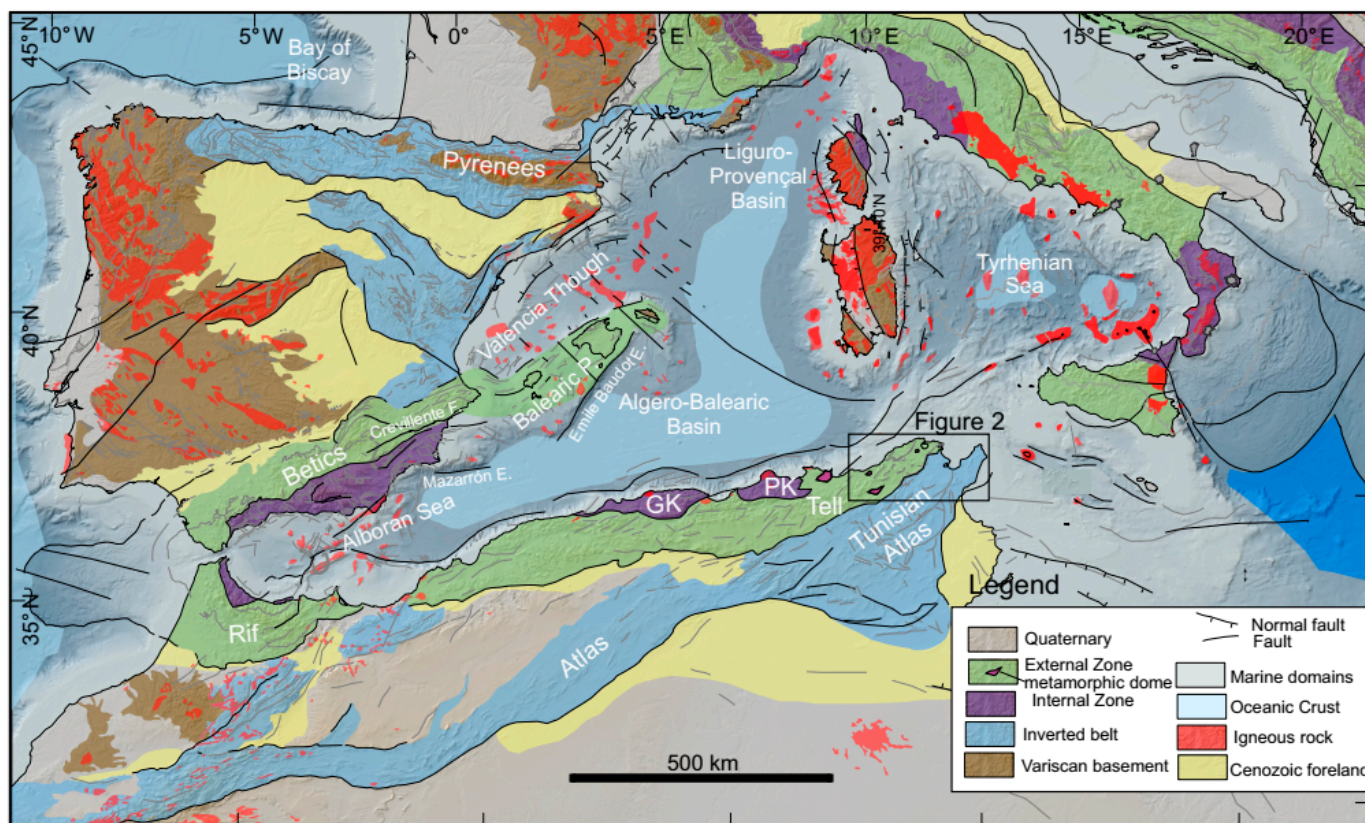


Figure 1. Tectonic sketch of the western Mediterranean basins and orogens. Modified from [31]. The box shows the Nappes zone location.

The present-day relief of the Maghreb-Betic orogen evolved in the context of the Cenozoic Eurasia-Africa collision [30,35,36] with the contribution of other mechanisms including Neogene extension [9,10,34,37–40] driven primarily by deep mantle tectonic mechanisms [8,18,41–43], dynamic topography due to slab pull and small-scale mantle upwelling and flow [3,19,44–46], magmatic crustal accretion at volcanic arcs [9,31,47], and recent contractional inversion [48–55]. The structure of the Atlas system is influenced by the inversion of Early Mesozoic rifting faults of both the Central Atlantic and Alpine Tethys [56].

The convergence of the Africa and Eurasia plates since the Late Cretaceous [57,58] led to oceanic subduction and associated early Eocene metamorphism (with rutile U-Pb ages of 49 Ma) in the Tell Triassic dolerites [10], Kabylean flysch, and associated serpentinites [35,59]. This compressional tectonic event was followed by early Oligocene continental subduction, resulting in ultrahigh-pressure (UHP) metamorphism in the African lower crust exhumed at the Edough Massif, dated by rutile U-Pb at 32 Ma [60,61]. Crustal thickening also induced high-pressure/low-temperature (HP-LT) metamorphism in hinterland units of the Alboran domain, with $^{40}\text{Ar}/^{39}\text{Ar}$ white mica dating yielding ages of 38–28 Ma [62,63]. The southeastward propagation of crustal thickening during the late Oligocene to early Miocene occurred concurrently with the extensional collapse of the over-thickened lithosphere in a back-arc supra-subduction setting, accompanied by associated tholeiitic and calc-alkaline magmatism [38,64–66].

Northern Tunisia is part of the Maghrebian chain, which is characterized by two distinct external domains: the Tellian Numidian zone (Nappes zone) in the north [67] and the highly folded domain with NE-SW-trending Triassic outcrops, known as the Diapirs zone, in the south (Figure 1). The deformed Tunisian Foreland lies further south in a more external position. The Tellian zone in northern Tunisia consists of sedimentary and low-

grade metamorphic rocks ranging in age from Triassic to Miocene [10,68]. The magmatic evolution of the Tellian zone includes scattered outcrops of intrusive felsic and mafic igneous rocks, related to the Alpine orogeny and emplaced in the La Galite, Mogods, and Nefza areas during the Serravallian to Messinian [28,69].

3. Geological and Geodynamic Settings of the Nappes Zone

The Nappes zone includes the Oligocene-Miocene Numidian Flysch, overlying Tellian and Atlas Mesozoic and Cenozoic sedimentary series from the North Maghreb passive margin ([23,67,70–73] Figure 2). It primarily features Triassic to Burdigalian imbricated allochthonous nappes [9,10,74] and metamorphic flysch successions on the la Galite Island (North of Tunisia) and NE Algeria [35,75–77]. Neogene extensional basins, such as the Oued Douimis, Mejerda, and Mateur basins, with a thickness reaching up to 1300 m, are present [9,10,78]. The Tellian units from top to bottom and from north to south include the Col de l'Adissa, Ain Draham, Jebel Ed Diss, and Kasseb units, spanning from Maastrichtian to Oligocene ([35,79]; Figure 2).

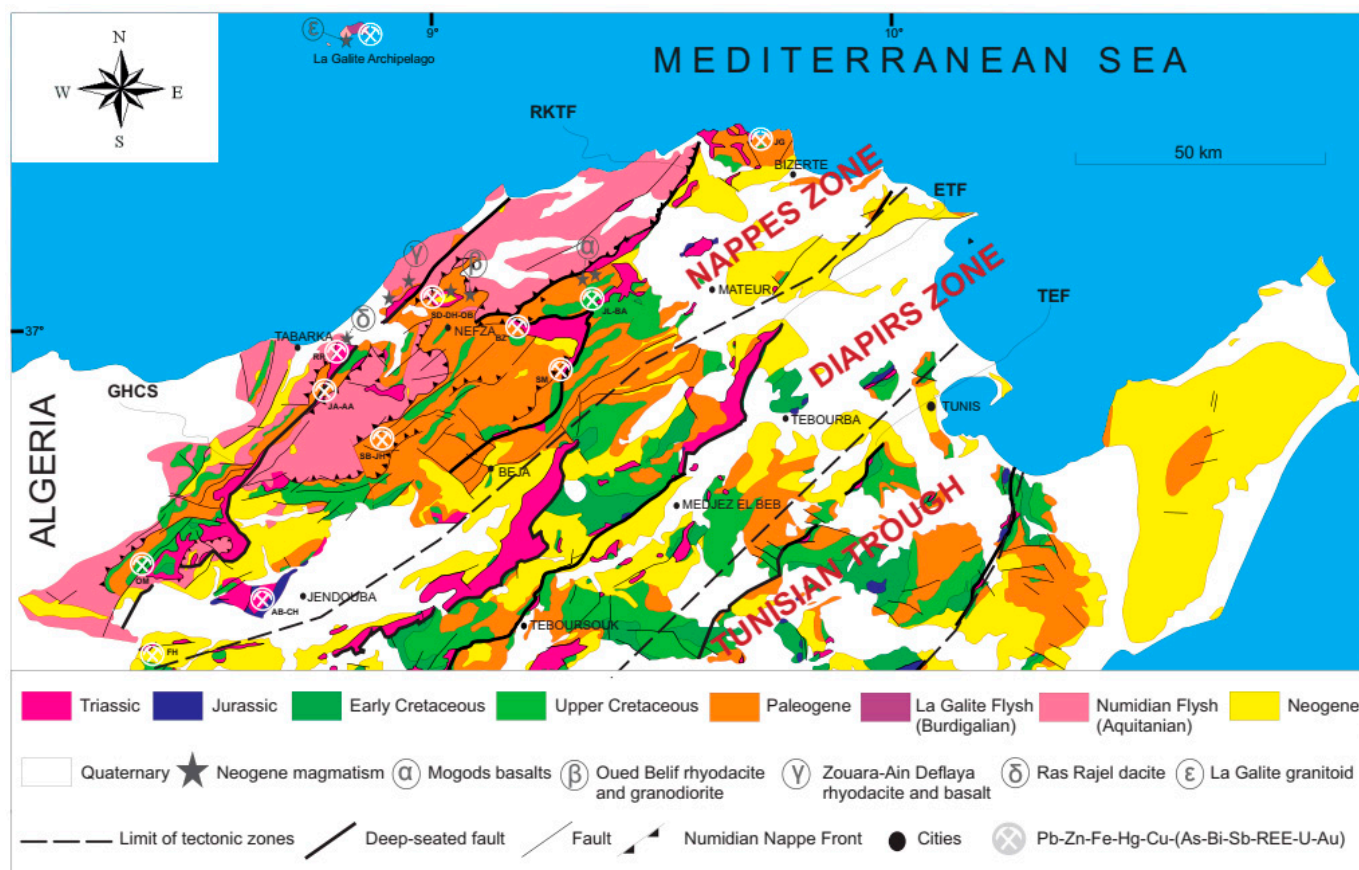


Figure 2. Simplified geologic map of northern Tunisia (modified from [71–73]) with the distribution of ore deposits, magmatic rocks, and deep-seated faults. GHCS: Ghardimaou-Cap Serrat Fault. RKTf: Ras el Korane-Thibar Fault. ETF: El Alia-Teboursouk Fault. TEF: Tunis-Elles Fault. SD-DH-OB: Sidi Driss-Douahria-Oued Belif, JA-AA: Jebel Arja-Ain Allega, RR: Ras Rajel, OM: Oued Maden, FH: Fedj Hassene, AB-CH: Ain el Bey-Chouichia, SB-JH: Sidi Bouaouane-Jebel Hallouf, BZ: Bazina, SM: Semmene, JL-BA: Jalta-Bir Afou, JG: Jebel Ghozlane.

The Nappes zone is cut by deep NE-SW faults bounding Tortonian-Messinian semi-grabens with km-scale displacements that exhumed the Tellian footwall series ([9,10,80–82]; Figure 2). Pliocene-Quaternary reactivation as reverse faults [83], along with E-W dextral and NE-SW sinistral faults, modified the fault systems of Northern Tunisia [78,79,84,85].

The Cap Serrat-Ghardimaou NE-SW Fault [86,87] in the Nefza region, extending over 70 km, exhumes Triassic outcrops beneath tilted Numidian Oligocene to early Miocene sediments [9] and shows Neogene volcanic extrusions such as Ras Rajel [87,88] with larger underlying magmatic bodies [69]. It is linked to Messinian high-angle extensional faults [9,10].

Neogene geodynamics of Northern Tunisia is influenced by NW-SE Africa-Eurasia convergence and slab rollback with back-arc basin opening [1,9,10,78,89,90]. Evidence of lithospheric delamination or detachment under the Tunisian Tell includes Serravallian-Tortonian and Messinian calc-alkaline rocks [29,91,92], rapid crustal exhumation [9,10,93], low-velocity mantle at depths of 50–100 km below NE Algeria and Northern Tunisia [2,11,86–96], and Neogene crustal thinning with anomalous high-velocity lower crust [97], which is interpreted as underplated Neogene mafic magmatic rocks [10]. Furthermore, the occurrence of SE-directed escape of the Tunisian Tell and Atlas, bounded by right-lateral strike-slip faults, is interpreted as a Subduction Transfer Edge Propagator fault system along the Southern Tunisian Atlas [9,98,99]. This region of anomalous low-velocity upper mantle shows significant Miocene Pb-Zn-Fe hydrothermal mineralization, with minor Hg, Au, and Sb [21,23,26–28,86,100–104].

Late Miocene-Pliocene extensional events during the Africa-Eurasia convergence led to half-grabens formation, fault reactivation, and bimodal magmatism with mafic lavas (7–8.5 Ma) and rhyodacite-granodiorite (8.5–12.5 Ma) in northern Tunisia [9,92]. In the later Plio-Quaternary period, there was northwest to Southeast-directed shortening, leading to the creation of inversion arrowhead structures, reverse faults, refolded extensional rollover anticlines, and folding of the older extensional faults.

Neogene magmatism in Northern Tunisia is attributed to subduction and slab delamination processes [42,105,106], as confirmed by tomography showing a detached slab beneath Tunisia [94,97], separated from the underlying lithosphere at a depth of 150 km since the late Miocene [94,107]. Other tomographic models show the slab extending even deeper, overlying the 660 km discontinuity [108]. This body has been interpreted as being formed from a stripped subcontinental lithospheric mantle attached to the African continental lithospheric mantle [109]. The continental nature of this slab would also explain the fact that the slabs imaged by [94] represent an area larger than the possible oceanic slab consumed by subduction since the Cretaceous [33].

Magmatic activity in the Nappes zone was initially calc-alkaline, with a subduction-related signature, then, transitional mafic lavas, with a double signature of both intraplate and orogenic magmatism [92]. These are related to an extensional post-collisional regime [92]. This evolution has been related to the progression of slab breakoff after tectonic collision [2]. The magmatic activity is differentiated into four groups ([28,70,74,92,110–112]; Figure 2). The first group (middle-late Miocene phase) includes calc-alkaline rhyodacites and granodiorites (12.9–8.2 Ma; [91]), and small lava flows (8.4–6.6 Ma; [87,91]) along the ENE-WSW-trending Oued Belif fault, Nefza Basin. They are present in Oued Belif (enclosing the Ragoubet el-Alia granodiorite and the Ragoubet Es-Seid) and also found in Ain El Araar rhyodacites), Ain Deflaïa, Jebel Haddada, and Oued Zouaraa. The second group (late Miocene) comprises Mogods basalts. They consist of basaltic dykes and necks in the Guelb Saad Moun (7–5.17 Ma; [87,91]) and rare basaltic lava flows and dykes in the Oued Melah (6.9 Ma; [87]). The third group (late Miocene) involves Mokta el-Hadid basalts (6.9 Ma; [28]) and Ras Rajel dacitic breccias [103], both emplaced along the NE-SW Guardimaou-Cap Serrat fault. Lastly, the fourth is marked by a middle-late Miocene granitoid batholith (14–10 Ma; [91]) in La Galite Archipelago [76,113].

It is worth mentioning that the first phase shows a component of lower-crustal melting due to lithospheric delamination after the Tethyan slab roll-back [114,115]. Conversely,

the second and third phases are attributed to an extensional post-collisional environment [92], while the fourth group is associated with an extensional tectonic event resulting from slab break-off [76,77]. The observed temporal evolution could also be linked to a slab break-off process [114,115] or lateral slab tearing and inboard subcontinental mantle delamination [9,10].

4. Characteristics of Major Polymetallic Mineralization of the Nappes Zone

The types and age range of magmatism, mineralization types, and isotopic compositions of ore districts in the Nappes zone are compiled in Figure 2 and Table S1 [20–22,24,25,27,28,86,101,103,104,116,117]. These deposits can be divided into five groups of ore zones or districts:

(i) Vein-Type Hydrothermal Copper sulfide deposits associated with the Neogene calc-alkaline rocks in the La Galite Archipelago. They are located within the internal zone of the Maghrebian Chain and belong to the crystalline massif zone [118]. Located 45 km off Cap Serrat and 60 km north of the town of Tabarka in the Sardinia-Tunisia Channel [76], La Galite deposit is of vein and fracture-filling type [102]. The Cu–Fe–Sb–Bi mineralization is hosted by diorites, granodiorites, microgranites, and granites, which formed during the middle to late Miocene and is associated with the La Galite ENE-WSW deep-seated fault [102,119].

(ii) The Ghardimaou-Cap Serrat ore deposit (GCSOD) is associated with late Miocene extensional faults, including the low-angle Nefza detachment, which is folded in the Oued Belif dome, and high-angle normal faults such as the Ghardimaou-Cap Serrat fault. These faults exhumed the Tellian units from under several kilometers of Numidian Flysch [9,10]. The activity of these faults also was coeval to Neogene magmatism, including the Ain Deflaia rhyodacite, Ras Rajel dacitic breccias, and Zouaraa rhyodacitic ignimbrites and basalts, and also facilitated the diapirism of Triassic evaporites. Notably, the Ras Rajel Fe oxides-(Ag-Au) deposit is the only occurrence directly associated with magmatic outcrops along the Ghardimaou-Cap Serrat fault. This deposit, found in the dacitic breccias, contains up to 48 g/t Ag, 0.3% Zn, 0.5% Pb, and 52 ppb Au, as reported by [116]. The deposits of the GCSOD are characterized by two major types of mineralization: mixed type and MVT (e.g., [102,105]). The primary ore deposits are polymetallic, featuring elements such as Hg-Pb-Zn-As-Sb-Cu of Oued Maden mixed type, MVT of Jebel Arja [28,86,101], MVT Zn-Pb-(Ba-Sr) of Ain Allega [101,104], and Zn-Pb-(Fe-As-Hg-Ba) MVT of Fedj Hassene [27,101].

(iii) The Nefza ore deposit (NOD) is marked by a suite of Pb-Zn-Fe-REE polymetallic mineralizations, associated with magmatism and hosted by Mio-Pliocene volcano-sedimentary and Messinian–Zanclean siliciclastic rocks filling semigrabens. These deposits include the IOGC of Oued Belif-Boukhchiba Fe-REE-U-Zn-Pb-(Au) mineralization [20], the Oued Belief Fe ores skarn [20,120], and the Messinian Zn-Pb-(Ba-Sr) SEDEX deposits of Sidi Driss and Douahria [21].

(iv) The Neogene basin ore deposits (NBOD), located on the edge of the Mogods, are characterized by a series of small polymetallic ore deposits scattered along and near the Bled El Aouana-Bizerte Fault [81,115]. The formation of these ore deposits is linked to Miocene extensional faults, such as the Ghezala low-angle normal fault. Some ore deposits are found near basalt lava flows and dyke outcrops in Guelb Saad Moon, Oued Melah, Jebel Jebes, and Jebel Sboua. These MVT mineralizations are hosted in Mio-Pliocene conglomerates with Pb-Zn-(Ba-As) at Jalta and Semene [23,26,121], which are cut and tilted over the Ghezala low-angle normal fault [9]. Other host rocks include Cretaceous carbonates with Pb-Zn-(F-Cu) at Kef El Fadjel and with Fe-Pb-Zn of El Ghreffa [122], Triassic dolostones with Pb–Zn at Jebel Zebs and Bazina [122], and in Eocene carbonates

with Pb-Zn of Jebel Ghozlane [23,24]. Additional Pb-Zn-(As-Sb) mineralizations occur without magmatic rock outcrops. These MVT deposits are hosted in lacustrine limestones and continental conglomerates of the Mejerda late Miocene extensional basin at Sidi Bou Aouane and El Haouaria in Beja [100,102], as well as in Late Cretaceous at Jebel Hallouf, and Khanguet Kef Tout [27,121].

(v) The El Haïrech-Ichkeul ore districts (HIOD) occur in the footwall and fault rock of extensional detachments that contributed to the exhumation of mid-crustal rocks in the core of the massifs [10]. Mixed type Fe-Cu rich-sulfides and Au mineralization at Ain El Bey, Chouichia, and Kef El Agueb deposits occur in the HIOD along faults that bound metamorphic outcrops of the early Mesozoic series of the Jebel el Haïrech and Fe-Cu of Jebel Ichkeul [102,123]. The Chouichia, Kef El Agueb, and Ain El Bey mineralizations are hosted along faults that cut through marine Eocene limestones, Oligocene-Miocene silty clays, and sandstones, as well as in the unconformably overlying sandstones [123]. The paragenesis consists of siderite-ankerite (gangue), pyrite, marcasite, arsenopyrite, and various copper sulfides [117,123].

The study of fluid inclusions in gangue minerals (quartz, fluorite, dolomite, siderite, calcite) from ore deposits (GCSOD, NOD, NBOD, HIOD) reveals ore-forming fluids with a wide range of temperature (110–300 °C) and salinity (23.2–42 wt% NaCl), responsible for the deposition of sulfides and sulfosalts containing Cu, As, Sb, Bi, and Ni [101,120,122]. These fluids were responsible for the genesis of various ore deposit types [101,117,120,122].

5. Methodology

For Pb isotope measurements, 2–3 mg of galena sample was dissolved using ultrapure (double distilled) HCl. The Pb isotope compositions were analyzed using a Nu Instruments™ multi-collector inductively coupled plasma mass spectrometer instrument within the Radiogenic Isotope facility at the University of Bern (Switzerland). Sample aliquots were subsequently mixed with ~1.5 mL of a 2% HNO₃ solution spiked with the NIST SRM 997 Thallium standard (2.5 ppb), and aspirated (~100 mL/min) into the ICP source using an Apex™ desolvating nebulizer (Nu Instruments Ltd., Wrexham, UK). Simultaneous measurements of all the Pb and Tl isotopes and ²⁰²Hg ion signals were achieved by using seven Faraday collectors. The ²⁰⁵Tl/²⁰³Tl ratio was measured to correct for instrumental mass bias (exponential law; ²⁰⁵Tl/²⁰³Tl = 2.4262). Upon sample introduction, data acquisition consisted of 2 half-mass unit baseline measurements prior to each integration block and 3 blocks of 20 scans (10 s integration each) for isotope ratio analysis. ²⁰⁴Hg interference (on ²⁰⁴Pb) was monitored and corrected using ²⁰²Hg. At the beginning of the analytical session, a 25 ppb solution of the NIST SRM 981 Pb standard, which was also spiked with the NIST SRM 997 Tl standard (1.25 ppb), was analyzed. The external reproducibility of individual analytical sessions was ca. 1×10^{-4} .

For the genetic classification, the method for calculating $\Delta\gamma$ and $\Delta\beta$ according to [124] is ($\Delta\beta = [\beta/\beta M(t) - 1] \times 1000$; $\Delta\gamma = [\gamma/\gamma M(t) - 1] \times 1000$; $\beta = {}^{207}\text{Pb}/{}^{204}\text{Pb}$; $\gamma = {}^{208}\text{Pb}/{}^{204}\text{Pb}$; $\beta M(t) = 15.33$; $\gamma M(t) = 37.47$).

6. Lead Isotope Compositions

6.1. Signature and Sources of Metals

The Pb isotope data from 39 galena samples from the Nappes zone in Northern Tunisia, compiled from previous studies [20,23,24,26–28] and supplemented with new data (Ain Allega), are listed in Table S2 and displayed in traditional Pb isotope covariance diagrams (Figure 3). Pb isotope data from Miocene felsic magmatic rocks in the Nefza area, North Africa Neogene granitoids [28,125], and Miocene volcanic rocks of the Betics and Alboran Sea [126] are also plotted for comparison. The average crustal Pb growth curves from [127]

are included for reference in Figure 3. The Pb isotope ratios for all galena samples range from 18.695 to 18.894 for $^{206}\text{Pb}/^{204}\text{Pb}$, 15.660 to 15.686 for $^{207}\text{Pb}/^{204}\text{Pb}$, and 38.895 to 39.000 for $^{208}\text{Pb}/^{204}\text{Pb}$. The Pb isotope compositions of galena samples from each deposit group are homogenous, with narrow Pb isotope ranges (Figure 3, Table S2; [24,26–28]). However, when compared to each other, they show heterogeneity, as illustrated in the uraniumogenic and thorogenic diagrams (Figure 3).

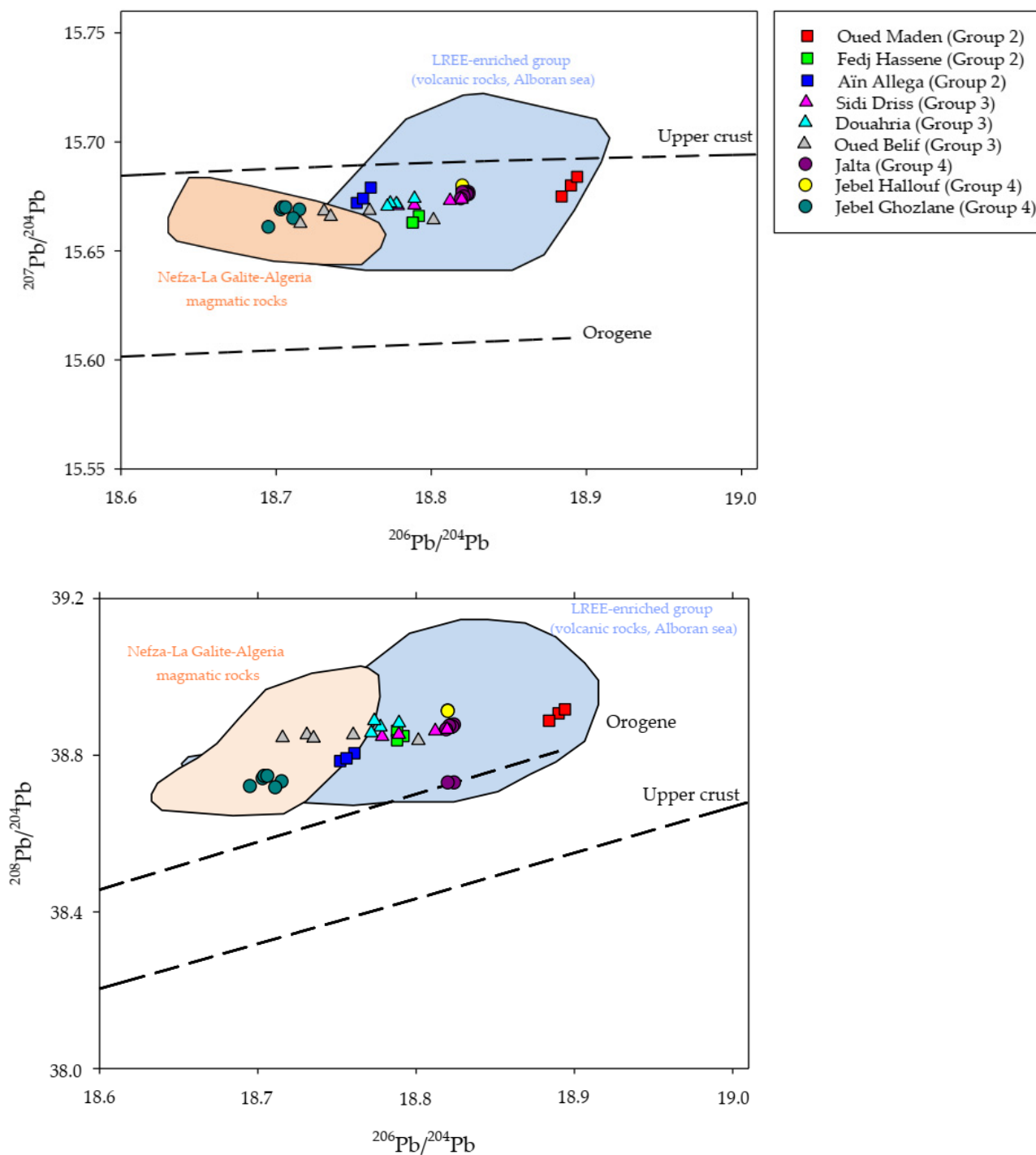


Figure 3. Lead isotope compositions of galena from selected Tunisian Nappes zone ore deposits plotted on $^{207}\text{Pb}/^{204}\text{Pb}$ vs. $^{206}\text{Pb}/^{204}\text{Pb}$ and $^{208}\text{Pb}/^{204}\text{Pb}$ vs. $^{206}\text{Pb}/^{204}\text{Pb}$ diagrams, together with Nefza-La Galite-Algeria Neogene magmatic rocks [28,125], and Alboran sea volcanic rocks [126]. Sources of data for Tunisian ore deposits (see Table S2).

All Pb isotopic data of all types align between the orogen and upper crustal curves of [127] (Figure 3) but are closer to the latter. This suggests that the Pb is derived from an upper crustal source [128]. The Oued Maden (Group 2, mixed type) deposit exhibits distinctly more radiogenic Pb isotope signatures, with high μ values (9.84), suggesting a greater contribution from evolved continental crustal materials. These signatures are consistent with fluids that may have leached metals from upper crustal reservoirs influenced by magmatic or hydrothermal processes. The crustal Pb isotopic signature could also reflect contributions from metamorphic fluids derived from deeper crustal levels presently exhumed by extensional faults in northern Tunisia. The involvement of various processes aligns with its classification as a mixed-type deposit, where metals are primarily sourced from the crust, but magmatic and metamorphic activity may have indirectly contributed by providing heat or fluids that facilitated the mobilization and transport of these metals [129]. In contrast, the Fedj Hassene and Ain Allega (Group 2) MVT deposits display less radiogenic Pb isotope compositions, indicating that the lead is derived from juvenile crustal reservoirs. The SEDEX type (Sidi Driss, Douahria; Group 3) deposits exhibit Pb isotopic signatures that overlap with both the MVT deposits (Fedj Hassene, Ain Allega, Jalta, Jebel Hallouf) and the magmatic field associated with the Nefza-La Galite-Algeria magmatic rocks and the LREE-enriched volcanic rocks of the Alboran Sea (Figures 3 and 4). This suggests a mixed source for the metals, where deep formational saline brines interacted with rock cover and basement, acquiring their isotopic signatures. Magmatic heat may have enhanced fluid circulation, facilitating the interaction of these saline fluids with various rock types. This is consistent with the SEDEX model, where metals are sourced from the basement and transported by brines into the sedimentary basin. The IOCG (Oued Belif (Group 3) also shows Pb isotopic signatures that primarily overlap with magmatic fields. This implies a potential influence from magmatic activity, possibly as a heat source or a minor metal contributor. The magmatic processes and fluid circulation driven by the Nefza extensional detachment may have provided the necessary conditions for the mobilization and transport of metals, highlighting the significant role of magmatism and hydrothermal activity in an extensional setting, typical in the genesis of these deposits.

The Pb isotopic composition of Jebel Ghozlane (Group 4) (MVT) stands out as the least radiogenic among the studied deposits. This suggests the involvement of crustal lead with a less evolved radiogenic signature, indicating a unique fluid pathway or source (i.e., unradiogenic lead) compared to other MVT and SEDEX deposits in the area.

The $\Delta\gamma$ - $\Delta\beta$ diagram (Figure 4) (with the detail of the calculation of $\Delta\gamma$ and $\Delta\beta$ is described in the method of [124]) shows that the calculated $\Delta\gamma$ and $\Delta\beta$ values for galena samples predominantly fall within the magmatic field (3a), corresponding to a mixed upper crust-mantle source characteristic of subduction processes (Figure 4). This suggests a magmatic-hydrothermal-metamorphism influence on the ore-forming systems in the study area. However, the involvement of other fluids, such as highly saline fluids typical of SEDEX systems and basinal brines typical of MVT systems, also contributed to ore deposition to varying degrees across different deposits. Magmatic centers, particularly active during the Miocene, may have served as primary drivers by providing heat that initiated the circulation of deep-seated saline and basinal brines within sedimentary basins. These brines could have scavenged metals from sedimentary or basement rocks, contributing to ore deposition. Moreover, the overlap of Pb isotope compositions with the field of Nefza-La Galite-Algeria Neogene magmatic rocks, as well as the middle to late Miocene LREE-enriched volcanic rocks of the Alboran Sea, further supports a magmatic influence. This overlap suggests that a magmatic source either directly contributed metals or facilitated the flow of fluids, which passed through various rocks and scavenged metals from magmatic sources (Figure 4). The Pb-Sr-Nd of La Galite-Algeria granites suggest

mixing processes involving anatectic melts and differentiated Island Arc-type magmas or melting of crustal terranes intruded by mantle-derived igneous rocks [125]. The Nefza granodiorites and rhyodacites, as highlighted by [28,106], exhibit enrichment of LILE, LREE, Pb, and W, indicative of felsic magmatism driven by calc-alkaline magma mixed at depth with predominant peraluminous crustal melts in post-collisional conditions [28,114]. Such magmatic systems likely provided both metals and the thermal energy required to drive fluid circulation. Additionally, the LREE-enriched volcanic rocks of the Alboran, enriched in fluid-mobile elements such as Rb, Th, U, K, and Pb, may have formed [126] through the mixing of MORB melts with 10–50% crustal melts, as represented by the cordierite-bearing volcanic rocks from southern Spain or through the addition of sediment melts to the mantle source.

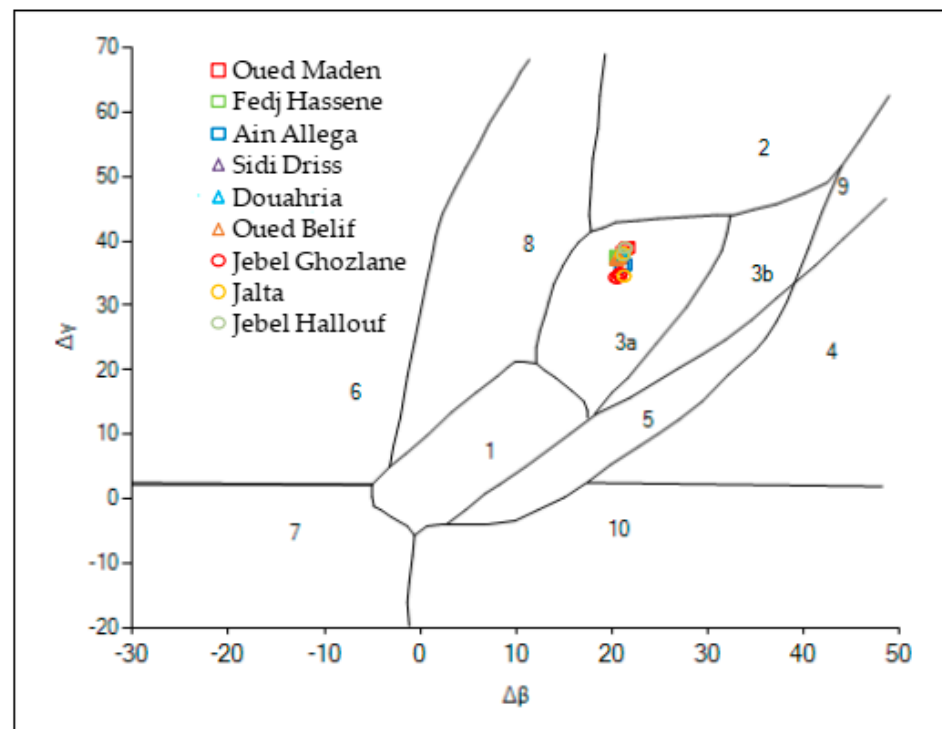


Figure 4. $\Delta\gamma$ - $\Delta\beta$ genetic classification diagram after [124] showing lead isotope composition of Nappes zone ores (1: mantle lead, 2: upper crustal lead, 3: mixed upper crustal and mantle lead-3a: magmatism, 3b: sedimentation, 4: chemical deposit lead, 5: submarine hydrothermal lead, 6: medium-high grade metamorphic lead, 7: hypometamorphic lower crustal lead, 8: orogenic belt lead, 9: ancient shale upper crustal lead, and 10: retrograde metamorphic lead) ($\Delta\beta = [\beta/\beta M(t) - 1] \times 1000$; $\Delta\gamma = [\gamma/\gamma M(t) - 1] \times 1000$; $\beta = {}^{207}\text{Pb}/{}^{204}\text{Pb}$; $\gamma = {}^{208}\text{Pb}/{}^{204}\text{Pb}$; $\beta M(t) = 15.33$; $\gamma M(t) = 37.47$).

Lead isotope data for ore deposits from the Tunisian Nappes zone are also plotted in Figure 5, alongside comparative data from (1) Algerian Tell ores [130], (2) the Morocco Rif ore deposits [131], and (3) ore deposits from southeastern Spain [132]. The Pb isotope compositions of the Nappes zone ores show strong similarity to those of the Algeria-Morocco Tell-Rif ores and southeastern Spain ones, suggesting comparable metal source and fluid pathways.

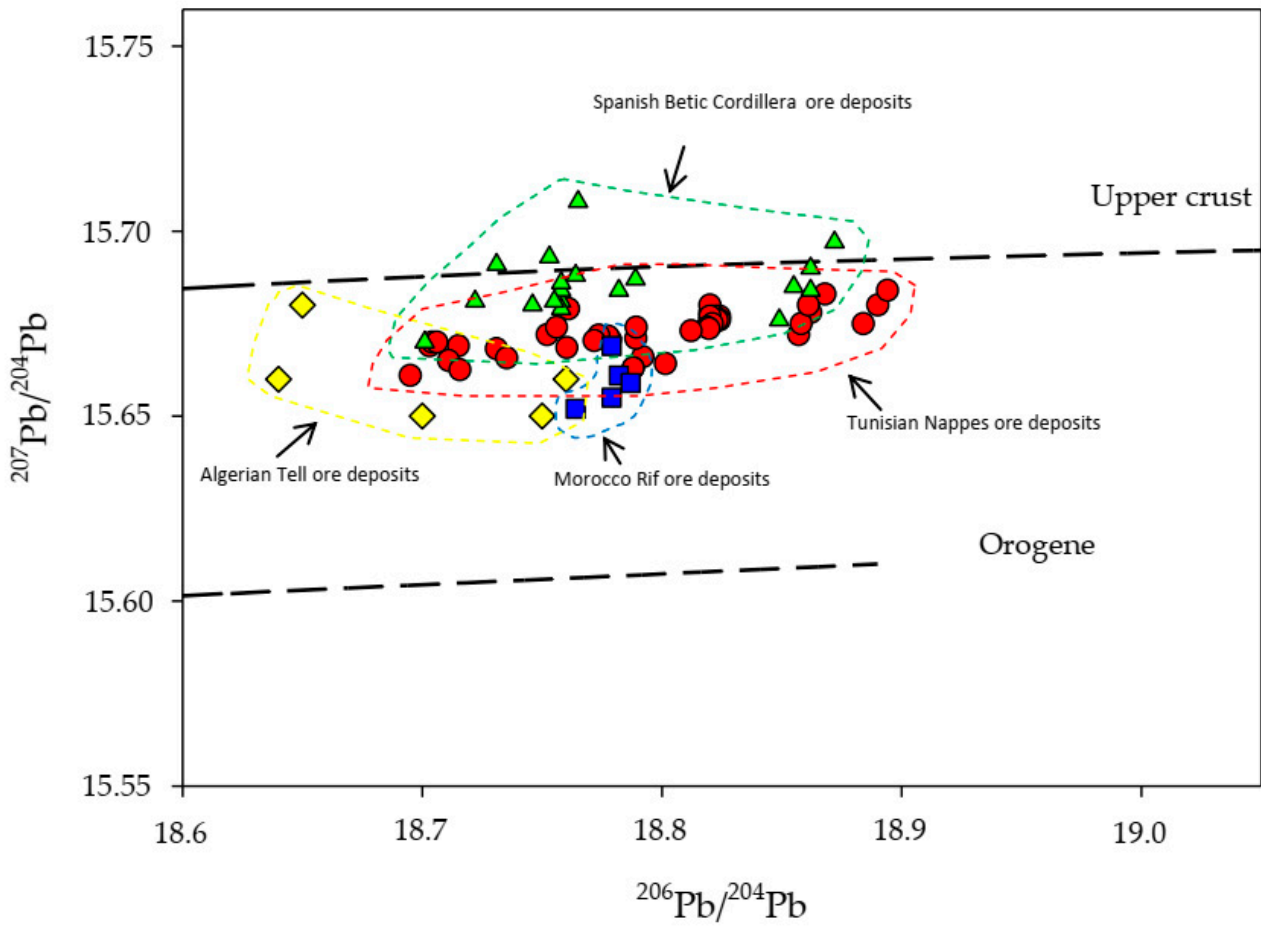


Figure 5. Lead isotope compositions of galena from selected Tunisian Nappes zone ore deposits plotted on a $^{207}\text{Pb}/^{204}\text{Pb}$ vs. $^{206}\text{Pb}/^{204}\text{Pb}$ diagram for comparison together with the ores of Algerian Tell [131], Morocco Rif [132], and southeastern Spain [133].

The calculated average values $^{238}\text{U}/^{204}\text{Pb}$ ($\mu = 9.50$), $^{232}\text{Th}/^{204}\text{Pb}$ ($\omega = 36.86$), and $^{232}\text{Th}/^{238}\text{U}$ ($\kappa = 3.88$) for the galena samples from the Nappes zone ore deposits, relative to the equation of [133], indicate notable deviations from the average crustal Pb evolution curve ($\mu = 9.74$, $\omega = 36.84$, and $\kappa = 3.78$; [134]). Specifically, the μ values are slightly lower, while the ω and κ values are higher. This suggests that the metals originated from a hybrid source, involving contributions from both the mantle and a dominant crustal component. The high $^{207}\text{Pb}/^{204}\text{Pb}$ ratios (>15.55) observed in these deposits provide further support for a predominantly upper continental crust origin for Pb [135], consistent with the findings from $\Delta\gamma$ – $\Delta\beta$ diagrams.

As shown in Figure 6A, there is a positive correlation between $^{207}\text{Pb}/^{204}\text{Pb}$ and μ , suggesting spatial and temporal variation in Pb sources. For example, deposits in the Oued Maden region (SW) exhibit higher $^{207}\text{Pb}/^{204}\text{Pb}$ and μ values, reflecting a more evolved lead source with a stronger upper crustal component [136]. In contrast, deposits in the NE, such as those in the Jebel Ghozlane and Nefza districts, show lower μ values, indicative of a less evolved source with possible mantle-derived contribution and/or a reservoir of low Pb radiogenic signature. Further analysis, presented in Figure 6B, reveals a strong correlation between μ values and model ages of mineralization, indicating that variations in $^{207}\text{Pb}/^{204}\text{Pb}$ and μ are primarily time-dependent, i.e., lead source evolved over time. These findings suggest that as the tectonic system evolved, Pb isotope compositions became increasingly influenced by upper crustal sources, resulting in more radiogenic signatures in younger mineralization. Despite the dominance of upper crustal signatures, some

deposits with lower μ values point to a mantle influence and/or a reservoir of unradiogenic crustal signature, highlighting the complexity of the metal sources in the region. Two potential sources for this unradiogenic lead are the young Miocene felsic rocks and mafic rocks. This hybrid system, involving contributions from both magmatic and crustal sources, is consistent with the broader regional context described in the Pb isotope and $\Delta\gamma$ - $\Delta\beta$ diagrams.

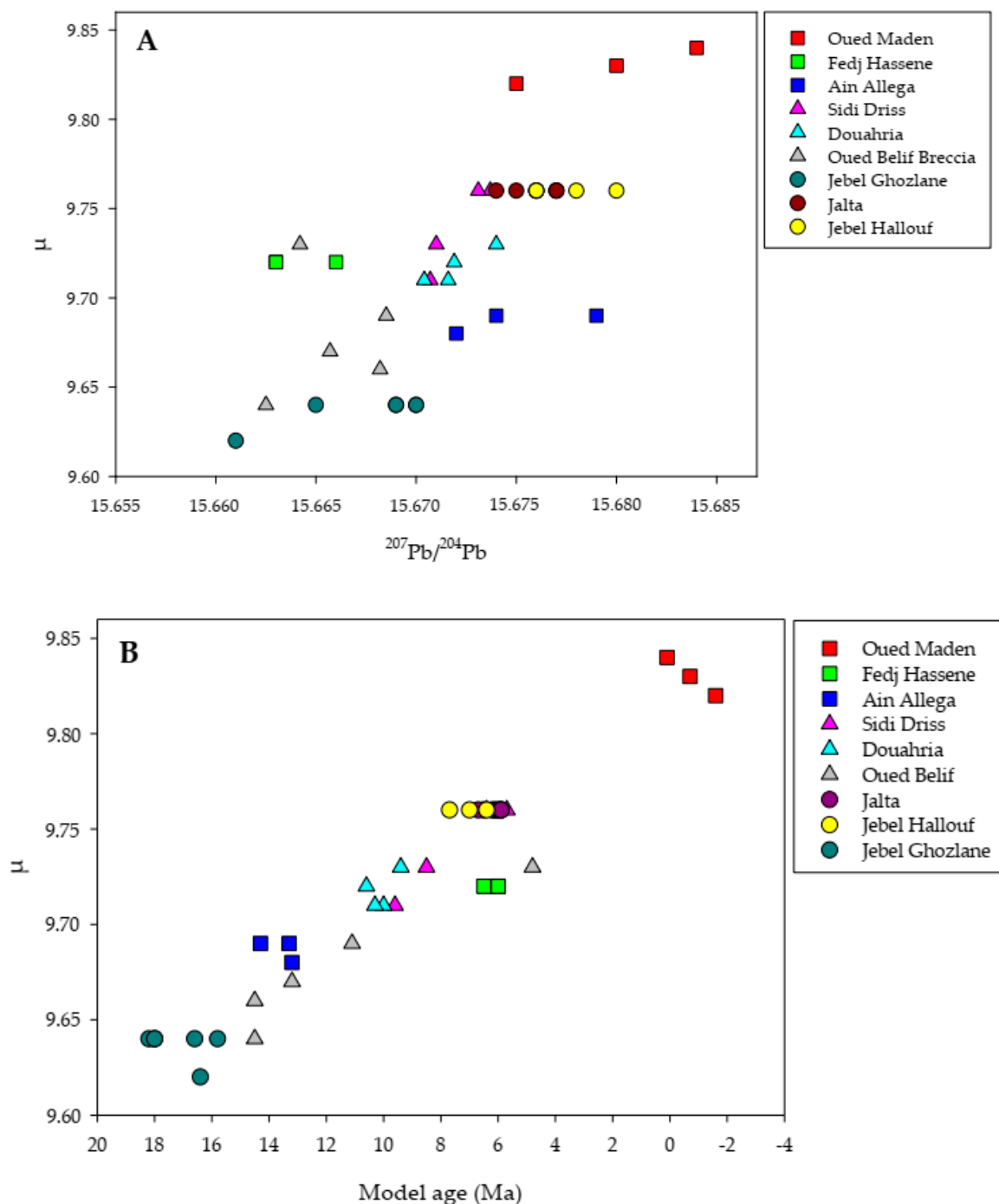


Figure 6. Scattergrams for the Nappes zone ore deposits, showing relationships between (A) $^{207}\text{Pb}/^{204}\text{Pb}$ and μ , and (B) model age and μ . Model ages and μ were calculated using the equation of [133].

While Pb isotopic variations provide an insight into the sources of metals, mineral paragenesis offers complementary evidence on the redox conditions under which these

metals were transported and deposited. The mineral paragenesis across the studied deposits (Table S1) provides valuable insights into the oxygen fugacity (fO_2) conditions during ore formation, highlighting distinct redox environments. IOCG deposits, such as Oued Belif, are characterized by oxidized conditions (high fO_2), as indicated by the dominance of hematite and goethite, which suggest a strong influence of magmatic-hydrothermal fluids. In contrast, SEDEX and MVT deposits, such as Sidi Driss, Ain Allega, and Fedj Hassene, formed under reduced conditions (low fO_2), as evidenced by sulfide-dominated assemblages, including galena, sphalerite, and pyrite, typical of basinal brines. Mixed-type deposits, such as Oued Maden and Chouichia-Ain el Bey, exhibit intermediate redox conditions, reflected in the coexistence of sulfosalts (e.g., tetrahedrite) and arsenopyrite. These variations in fO_2 align with the broader tectonic and magmatic framework, where mantle delamination and crustal extension generated the thermal and structural conditions to drive diverse fluid systems, accommodating both oxidized magmatic fluids and reduced basinal brines. Together, these observations emphasize the critical role of fO_2 in controlling mineral assemblages and ore-forming processes across the region.

6.2. Pb-Pb Age Dating of Ores

The extraction time of lead from its reservoir can correspond to the crystallization time of Pb-rich minerals, such as galena. Therefore, the model age can reflect the timing of ore genesis. This assumption holds true because most ore deposits are hosted in Miocene rocks, where reworking of lead sources is minimal, supporting the concept of a closed system during mineralization. The model ages of polymetallic ore deposits associated with the Ghardimaou-Cap Serrat Fault (e.g., Fedj Hassene, Ain Allega, and Oued Maden mineralizations) average 6.10 Ma, 13.6 Ma, and -0.73 Ma, respectively (Table S1). The Fedj Hassene ores correspond to the late Tortonian-Messinian age, consistent with the age of basalts in nearby basins such as Mokta el-Hadid, Boulanague, and Zouaraa Basin (8 ± 1 Ma: [89,137]; 8.4 ± 0.4 Ma: [91]; 6.6 Ma: [87]; Figure 7). Similarly, the Ain Allega mineralization aligns with a middle Miocene age (average 13.6 Ma), consistent with the emplacement of the La Galite granitoids (14–10 Ma; [91]; Figure 7). In contrast, the Oued Maden mineralization records negative model ages, which are likely due to the mixing of varying amounts of radiogenic lead into the system [138,139]. The Pb model ages of Zn-Pb-(Fe-Ba-Sr) deposits associated with Neogene magmatism (e.g., Sidi Driss, Douahria, and Oued Belif) range from 5.7 to 14.5 Ma, with an average value of 9.89 Ma (Table S2). These values align with the K-Ar age of 8–12 Ma for the Nefza felsic magmatic rocks ([91,137]; Figure 7) and the 9.1–9.4 Ma for the Oued Belif rhyodacite ([20]; Figure 7). Collectively, these data suggest a late Tortonian-early Messinian age for the remobilization of lead from source rocks and its fixation in galena, as confirmed by ([21,103]). The model age calculations for Pb-Zn-Ba-Sr-(As-Sb) deposits hosted in Neogene and Mesozoic carbonates and continental conglomerates (e.g., Jebel Hallouf, Jebel Ghozlane, and Jalta) range from 7 to 18.2 Ma (Table S2). Two distinct average model age values can be identified: 17.16 Ma for Jebel Ghozlane, corresponding to the early Miocene and 5.01 Ma for the remaining ore deposits Jalta and Jebel Hallouf, corresponding to the late Miocene-Pliocene. The 5.01 Ma age is consistent with the emplacement late Miocene to Pliocene Basaltic dykes and necks widely distributed across the Mogods area (e.g., Guelb Saad Moun: 7–5.17 Ma; ([68,87]; Figure 7); Oued Melah area: 6.9 Ma; [87]). The model Pb ages of galena of most deposits, except Oued Maden, align with the timing of magmatism in the Nappes zone during the late Miocene extensional event. This Miocene age is also consistent with other regional deposits, including the Tell Algerian ores [130], the Cabo de Gata deposits from southeastern Spain (9.2 Ma, [132]), and the Moroccan Rif Melilla-Nador peninsula deposits (7.8 Ma, [131]). The Miocene magmatism in the Nappes zone is interpreted to

have been derived from the subcontinental lithospheric mantle metasomatized during earlier subduction events and mixed with partial melts from the African crust [9,28,114]. This melting has been attributed to asthenospheric mantle upwelling due to lithospheric detachment [114] or delamination [5,9]. The subduction-related origin is further supported by the high $^{207}\text{Pb}/^{204}\text{Pb}$ values ($>15.65\text{--}15.71$) [47].

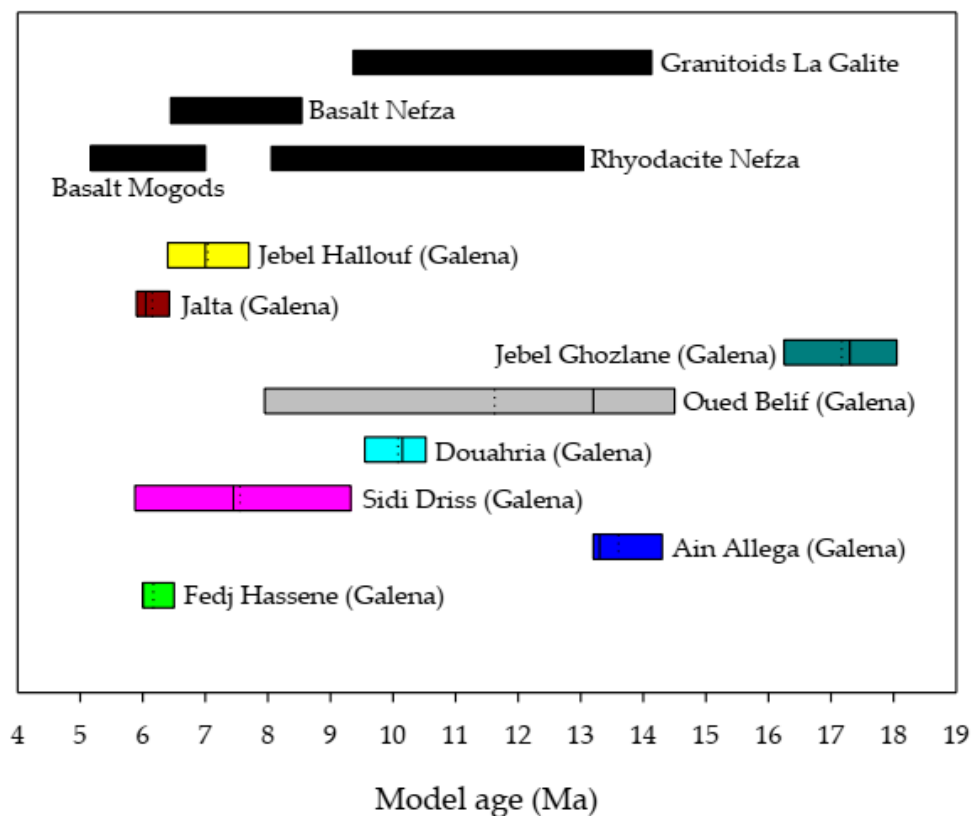


Figure 7. Model age distribution of galena ores [24,26–28] and magmatic rocks [28,87,91,104] of the Nappes zone. Dotted line corresponds to the mean value. The solid line corresponds to the outlier.

7. Evolution and Tectonic Model of the Nappes Zone Atlas Belt

The detachment of a subducted slab, leading to orogenic collapse, is a significant geological mechanism influencing mineralization in the Atlas Mountains of North Africa (Figure 8). This collapse occurs due to either the sinking of a thick, unstable lithospheric root or the detachment of a relatively cold subducted slab. In both scenarios, the subsequent rise of the hot asthenosphere into shallower depths enhances heat transfer within the continental lithosphere. This increased heat promotes the generation of felsic and mafic melts, intensifies fluid activity, and creates favorable geochemical conditions for the genesis of various ore deposit types (e.g., MVT, SEDEX, IOCG deposits; Figure 8). Slab detachment, followed by lithospheric delamination, is the primary driver behind the orogenic collapse, facilitating heat and fluid influx from the hot mantle wedge asthenosphere at shallower levels. This crustal-mantle interaction likely facilitated devolatilization in deeper regions, generating metamorphic fluids that contributed to ore-forming systems. These processes not only contribute directly to ore formation but also indirectly by driving hydrothermal fluid circulation, creating metal-enriched systems linked to regional tectonic activity. This tectonic mechanism explains the observed spatial correlation between late-stage mineralization, involving metals such as mercury, antimony, arsenic, copper, silver, and potentially gold, with areas of orogenic collapse and shallow, low-velocity mantle zones [2,11]. The Pb-Pb isotopic ages of ore deposits directly reflect these tectonic events.

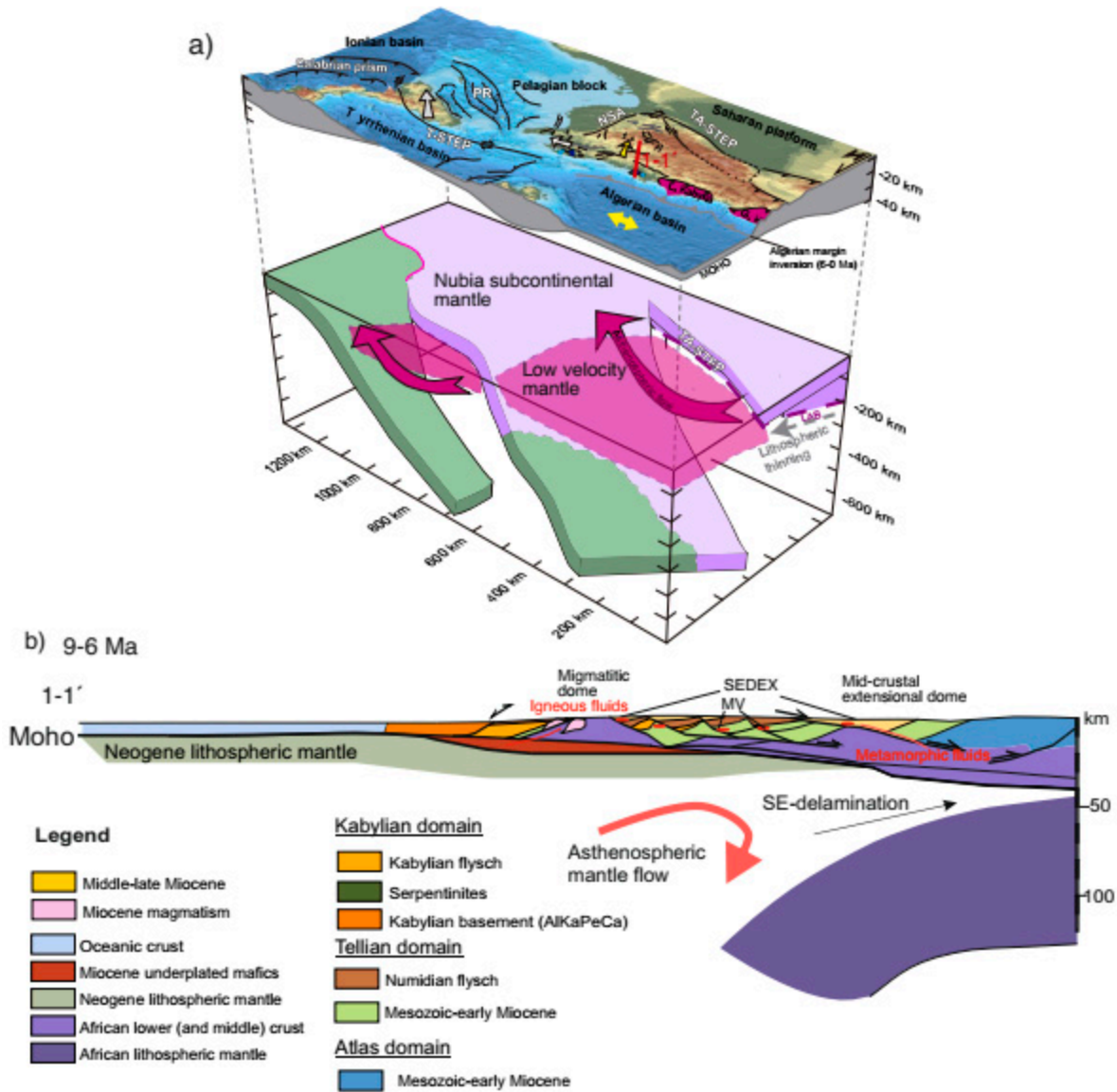


Figure 8. (a) Cartoon of the tectonic mechanisms driving lithospheric rejuvenation, crustal extension, magmatism, and associated metal endowment in Northern Tunisia and Algeria during the middle to late Miocene (b) Schematic cross-section 1-1' across Northern Algeria-Tunisia showing the driving mechanisms and tectonic setting of different ore deposits in the region at the time of deposition. Notice the North to South crustal thinning gradient, taken from the EGT'85 refraction seismic experiment (99), and the occurrence of magmatic outcrops and a high-velocity lower crustal domain that are present towards the North. NSA: North-South Axis. TA-STEP: Tunisian Atlas Step Fault. T-STEP: Tyrrhenian Step Fault. PR: Pantelleria rift. LAB: Lithosphere Asthenosphere Boundary.

The magmatic, mineralization, and tectonic events in the Nappes Zone Atlas (NZA) belt during Neogene times can be summarized as follows (Figure 8):

- Late Miocene extension and magmatism in the westernmost Mediterranean and Tell (~9–5 Ma): Throughout the Cenozoic, the Western Mediterranean experienced alternating extensional and shortening events, including in regions such as the Alboran domain, Valencia Trough, and Kabylies. Similar tectonic events likely occurred in northern Tunisia, with a potential crustal extension between Eocene and early Miocene shortening events or coeval with shortening in the footwall [10]. By Langhian-Serravallian times, as the E-W extension progressed in the Algerian basin [140], magmatism related to slab tearing propagated westwards and eastward along the Mediterranean

Maghreb margin [114]. Magmatism in northeastern Algeria and the Tunisian Tell between the early to late Miocene (16–6 Ma) likely involved significant mafic underplating under the northernmost coastal regions, as indicated by Vp velocities between 7.5 and 6.9 km/s at the base of the crust along the N-S EGT'85 line [97]. Concurrently, the Alboran volcanic arc formed with tholeiitic to calc-alkaline magmatism due to the eastward subduction of Tethys oceanic lithosphere beneath the Alboran basin [125,141,142]. During the Serravallian-Tortonian, slab tearing or break-off, along with related Si-K-rich magmatism, continued westward into the Rif and eastwards into the Tunisian Tell [10,127,142]. The magmatism persisted into the Tortonian-Messinian period [141,143], remaining active and widespread as extension neared its end. Polymetallic mineralizations in the Betics evolved during this late Miocene volcanic and extensional context [144]. This mineralization event is initially related to early Tortonian subduction calc-alkaline magmatism, exemplified by the Rodalquilar mine [145] and later associated with late Tortonian Si-K shoshonitic magmatism. Late Tortonian volcanogenic mineralizations in the Betics include the Herrerías Fe-Ba-Zn-Ag deposit [146,147]. This later magmatism, equivalent in age and context to the rhyodacitic magmatism of the Nefza district in Tunisia, has been associated with lower-crustal melting and mixing with mantle melts after subcontinental lithospheric delamination [9,10]. In the Tunisian region, polymetallic mineralizations were formed in the Nappes zone ore districts (GCSOD, NOD, NBOD, HIOD) during the development of late Miocene basins, coeval with active extension and associated magmatism. During the late Miocene (Tortonian-Messinian, 9–5 Ma), the NZA experienced extensive magmatism, especially in regions such as Nefza and Mogods. Pb isotope model ages for ore deposits along the Ghardimaou-Cap Serrat Fault system (e.g., Fedj Hassene), indicate ore emplacement around 6.1 Ma, concurrent with the late Miocene period of crustal extension and volcanic activity. These ages are consistent with the regional basaltic and felsic magmatism (8–6 Ma) recorded in nearby basins. Zn-Pb-Fe-Ba-Sr mineralizations at Sidi Driss, Douahria, and Oued Belif yield Pb isotope ages between 5.7 and 14.5 Ma, with an average of 9.89 Ma, matching the regional magmatic events (8–12 Ma) in the Nefza district. This further indicates that the ore deposits formed as part of a larger metallogenic event linked to Neogene magmatism. The Pb isotope ages of galena from other deposits, such as Jalta, Jebel Hallouf, and Jebel Ghozlane, range from 7 Ma to 18.2 Ma, with two distinct average values: 17.16 Ma (Early Miocene) for Jebel Ghozlane and 5.01 Ma (late Miocene-Pliocene) for Jalta and Jebel Halouf. The younger ages align with the final stages of extension and magmatism associated with basaltic dykes and volcanic necks widespread in the region, such as Guelb Saad Moun. Additionally, the first occurrence of intraplate alkaline volcanism that took place in the Atlas during this time is represented by the Siroua volcano.

- Tectonic inversion and magmatism: Extensional tectonics in the Western Mediterranean, primarily driven by slab dynamics, was followed by a post-late Miocene tectonic inversion of the Algerian basin margins due to continued NW-SE Africa-Eurasia convergence [53–55]. This inversion reactivated late Miocene normal faults as reverse faults, folding low-angle extensional systems in Tunisia during the Plio-Quaternary [9,84].

In conclusion, the delamination processes and associated slab dynamics in the Nappes zone created the thermal and geochemical conditions essential for various ore deposit types, either directly through magmatic and metamorphic activity or indirectly by driving fluid circulation and crustal extension. These processes define a metallogenic evolution strongly tied to regional tectonic, magmatic, and metamorphic events during the late Miocene.

8. Alpine Belt and Atlas Belt

The European Alpine Belt (EAB), which includes the Inner Carpathians and Basque-Cantabrian basin, and the Atlas Belt in Northern Tunisia, Algeria, and Morocco are integral parts of the Tethyan Zinc-Lead metallogenic province (e.g., [23,24,26,27,130–132]). These regions host numerous polymetallic deposits, making them part of one of the most significant metallogenic provinces globally [147]. Mineralization in these belts occurs within collisional orogens, where hydrothermal processes are associated with orogen-scale faulting in the upper, rigid part of Earth's crust. These faulting events, often linked to gravitational instability in subducted slabs during the waning phases of convergence, involve processes such as slab roll-back and slab break-off (e.g., [2,148,149]). Late Cenozoic mineralization, orogenic collapse, and slab detachment in the European Alpine Belt share similarities with the metallogenic evolution related to mantle delamination beneath Northern Tunisia during the Neogene. In the Alpine Belt, mineralization is primarily associated with extensional settings during the late stages of collision, often in the absence of significant contemporaneous magmatism [2]. Notable spatial associations exist between Late Cenozoic mineralization, regions of orogenic collapse, and underlying low-velocity mantle zones in the Alpine Belt [2,11]. This mineralization includes vein and replacement deposits of metals such as Hg, Sb, Au, Zn, Pb, and Ag, along with porphyry copper systems hosted within Late Cenozoic calc-alkaline to alkaline volcanic belts. The metallogenic evolution in Northern Tunisia during the Neogene is marked by late Miocene events, coinciding with lithospheric delamination and subduction-related mantle interactions (Figure 8). These processes created favorable geochemical and thermal conditions for ore genesis by driving mantle upwelling, fluid influx, and crustal extension, which directly or indirectly facilitated the mobilization and concentration of metals. Lead isotope signatures from galena samples in the Nappes zone provide key evidence linking mineralization to magmatic processes. Specifically, the Pb isotope data overlap with those of Neogene magmatic rocks in the Nefza region and the Alboran Sea, indicating significant mantle-crust interactions. This suggests that mantle-derived fluids and melts played a crucial role in the genesis of ore deposits. The comparison between the Alpine and Atlas belts reveals similarities in late-stage mineralization processes despite differences in their geological settings. Both regions display late-stage mineralization associated with extensional tectonics, closely linked to mantle mechanisms such as subduction, delamination, and/or slab detachment. Additionally, the spatial correlation between mineralization and orogenic collapse underscores the role of slab detachment in creating conditions conducive to ore formation. In Northern Tunisia, similar dynamics during the late Miocene facilitated ore formation. The Pb isotope compositions in Northern Tunisia indicate that metals were sourced from a mixture of upper crustal and mantle-derived magmas. However, as highlighted by the $\Delta\gamma$ - $\Delta\beta$ diagram (Figure 4), the isotopic data show a predominant upper crustal signature with a minor mantle-derived component. This pattern reflects a hybrid metallogenic process, where mantle contributions primarily acted as thermal and fluid drivers, while metals were predominantly sourced from the upper crust. This underscores the critical role of subduction-related mantle-crust interactions in ore formation, as observed in the European Alpine Belt during the Late Cenozoic. These findings highlight the complex interplay of tectonics, mantle-crust dynamics, and mineralization in ore formation and exploration.

9. Conclusions

The geological processes driving mineralization in the Tell-Atlas Mountains of North Africa are complex and multifaceted, encompassing a range of ore deposit types including MVT, SEDEX, and IOCG. Pb isotope compositions reveal a hybrid metallogenic system with metals primarily sourced from the upper crust with mantle contributions.

The Pb isotope overlap of all deposits with Neogene magmatic rocks and middle to late Miocene volcanic rocks suggests that these metals are linked to tectonic mechanisms such as slab tearing and delamination following the subduction of the Maghrebian lithosphere.

These mechanisms rejuvenated the lithosphere, leading to orogenic collapse, magmatism, and fluid circulation, driving magmatic-hydrothermal fluid systems through extensional faults and their interaction with cogenetic late Miocene sedimentary basins. This structural reorganization created pathways for the movement of basinal brines (MVT deposits) and saline fluids (SEDEX), alongside magmatic-hydrothermal fluids responsible for IOCG mineralization. The contribution of metamorphic fluids highlights the significance of extensional fault systems in the mobilization and transport of metals to depositional sites. This underscores the role of mantle-crust dynamics and highlights the significance of tectonic and fluid dynamics in ore genesis.

Overall, this study underscores the complex interplay between tectonics, mantle-crustal interactions, and mineralization events in the Tell-Atlas Mountains. Further research into the spatial and temporal evolution of these processes will deepen our understanding of mineralization dynamics and support the exploration of mineral resources in the region.

Supplementary Materials: The following supporting information can be downloaded at: <https://www.mdpi.com/article/10.3390/min15010031/s1>. Table S1. The main ore deposit distributions and characteristics of the Nappes zone; Table S2. Lead isotope composition of galena of the main Nappes zone ore deposits.

Author Contributions: Conceptualization, N.J.; Methodology, N.J.; Validation, N.J., F.S., L.R., E.J.C. and G.B.-R.; Writing—Original Draft Preparation, N.J.; Writing—Review and Editing, N.J., F.S., L.R., E.J.C. and G.B.-R.; Visualization, N.J., F.S., L.R., E.J.C. and G.B.-R. All authors have read and agreed to the published version of the manuscript.

Funding: GB is supported by the Ministry of Science and Innovation grant “LANDMARC” (PID2023-149821NB-I00) funded by MCIN/SRA (Spanish State Research Agency, <https://doi.org/10.13039/501100011033>, accessed on 16 December 2024).

Data Availability Statement: The original contributions presented in the study are included in the article/Supplementary Materials, further inquiries can be directed to the corresponding author.

Acknowledgments: We are grateful to four anonymous reviewers whose comments and suggestions improve the quality of this paper. We also appreciate the Associate Editor and Editor-in-Chief for the handling of this manuscript.

Conflicts of Interest: The authors declare no conflicts of interest.

References

1. Carminati, E.; Wortel, M.J.R.; Spakman, W.; Sabadini, R. The role of slab detachment processes in the opening of the western-central Mediterranean basins: Some geological and geophysical evidence. *Earth Planet. Sci. Lett.* **1998**, *160*, 651–665. [[CrossRef](#)]
2. De Boorder, H.; Spakman, W.; White, S.H.; Wortel, M.J.R. Late Cenozoic mineralization, orogenic collapse and slab detachment in the European Alpine Belt. *Earth Planet. Sci. Lett.* **1998**, *164*, 569–575. [[CrossRef](#)]
3. Duggen, S.; Hoernle, K.; Van den Bogaard, P.; Rüpke, L.; Phipps Morgan, J. Deep roots of the Messinian salinity crisis. *Nature* **2003**, *422*, 602–606. [[CrossRef](#)]
4. Wortel, M.J.R.; Spakman, W. Subduction and slab detachment in the Mediterranean-Carpathian region. *Science* **2000**, *290*, 1910–1917. [[CrossRef](#)]
5. Roure, F.; Casero, P.; Addoum, B. Alpine inversion of the North African margin and delamination of its continental lithosphere. *Tectonics* **2012**, *31*, TC3006. [[CrossRef](#)]
6. Chiarabba, C.; Giacomuzzi, G.; Bianchi, I.; Agostinetti, N.P.; Park, J. From underplating to delamination-retreat in the northern Apennines. *Earth Planet. Sci. Lett.* **2014**, *403*, 108–116. [[CrossRef](#)]
7. Thurner, S.; Palomeras, I.; Levander, A.; Carbonell, R.; Lee, C.T. Ongoing lithospheric removal in the western Mediterranean: Evidence from Ps receiver functions and thermobarometry of Neogene basalts (PICASSO project). *Geochem. Geophys. Geosyst.* **2014**, *15*, 1113–1127. [[CrossRef](#)]

8. De Lis Mancilla, F.; Booth-Rea, G.; Stich, D.; Pérez-Peña, J.V.; Morales, J.; Azañón, J.M.; Martin, R.; Giaconia, F. Slab rupture and delamination under the Betics and Rif constrained from receiver functions. *Tectonophysics* **2015**, *663*, 225–237. [[CrossRef](#)]
9. Booth-Rea, G.; Gaidi, S.; Melki, F.; Marzougui, W.; Azañón, J.M.; Zargouni, F.; Galvé, J.P.; Pérez-Peña, J.V. Late Miocene extensional collapse of northern Tunisia. *Tectonics* **2018**, *37*, 1626–1647. [[CrossRef](#)]
10. Booth-Rea, G.; Gaidi, S.; Melki, F.; Marzougui, W.; Ruano, P.; Nieto, F.; Azañón, J.M.; Galvé, J.P.; Hidas, K.; Garrido, C.J. Metamorphic Domes in Northern Tunisia: Exhuming the Roots of Nappe Belts by Widespread Post-Subduction Delamination in the Western Mediterranean. *Tectonics* **2023**, *42*, e2022TC007467. [[CrossRef](#)]
11. El-Sharkawy, A.; Hansteen, T.H.; Clemente-Gomez, C.; Fulla, J.; Lebedev, S.; Meier, T. Cenozoic volcanic provinces and shallow asthenospheric volumes in the Circum-Mediterranean: Evidence from magmatic geochemistry, seismic tomography, and integrated geophysical-petrological thermochemical inversion. *Geochem. Geophys. Geosyst.* **2024**, *25*, e2023GC011017. [[CrossRef](#)]
12. Menant, A.; Jolivet, L.; Tuduri, J.; Loiselet, C.; Bertrand, G.; Guillou-Frottier, L. 3D subduction dynamics: A first-order parameter of the transition from copper- to gold-rich deposits in the eastern Mediterranean region. *Ore Geol. Rev.* **2018**, *94*, 118–135. [[CrossRef](#)]
13. Neubauer, F.; Lips, A.; Kouzmanov, K.; Lexa, J.; Ivașcanu, P. 1: Subduction, slab detachment and mineralization: The Neogene in the Apuseni Mountains and Carpathians. *Ore Geol. Rev.* **2005**, *27*, 13–44. [[CrossRef](#)]
14. Holwell, D.A.; Fiorentini, M.; McDonald, I.; Lu, Y.; Giuliani, A.; Smith, D.J.; Keith, M.; Locmelis, M. A metasomatized lithospheric mantle control on the metallogenic signature of post-subduction magmatism. *Nat. Commun.* **2019**, *10*, 3511. [[CrossRef](#)]
15. Decree, S.; Van Ham-Meert, A.; Baele, J.-M.; Namur, O.; Deloule, E.; Marignac, C. Irish-type deposits in Tunisia: A new perspective to assign the Pb–Zn deposits of the Nefza District. In *Irish-Type Deposits Around the World*; Andrew, C.J., Hitzman, M.W., Stanley, G., Eds.; Irish Association for Economic Geology: Dublin, Ireland, 2023; pp. 393–406. [[CrossRef](#)]
16. Reynolds, N.A.; Allen, M.A.; Muhling, P.; Gianfriddo, C. Global Irish—Diversity of the diaspora. In *Irish-Type Deposits Around the World*; Andrew, C.J., Hitzman, M.W., Stanley, G., Eds.; Irish Association for Economic Geology: Dublin, Ireland, 2023; pp. 45–94. [[CrossRef](#)]
17. Schettino, E.; González-Jiménez, J.M.; Marchesi, C.; Palozza, F.; Blanco-Quintero, I.F.; Gervilla, F.; Braga, R.; Garrido, C.J.; Fiorentini, M. Mantle-to-crust metal transfer by nanomelts. *Commun. Earth Environ.* **2023**, *4*, 256. [[CrossRef](#)]
18. Govers, R.; Wortel, M.J.R. Lithosphere tearing at STEP faults: Response to edges of subduction zones. *Earth Planet. Sci. Lett.* **2005**, *236*, 505–523. [[CrossRef](#)]
19. Hidas, K.; Garrido, C.J.; Booth-Rea, G.; Marchesi, C.; Bodinier, J.L.; Dautria, J.M.; Louni-Hacini, A.; Azzouni-Sekkal, A. Lithosphere tearing along STEP faults and synkinematic formation of lherzolite and wehrlite in the shallow subcontinental mantle. *Solid Earth* **2019**, *10*, 1099–1121. [[CrossRef](#)]
20. Decrée, S.; Marignac, C.; De Putter, T.; Yans, J.; Clauer, N.; Dermech, M.; Aloui, K.; Baele, J.M. The Oued Belif hematite-rich breccia: A Miocene iron oxide Cu–Au–(U–REE) deposit in the Nefza mining district, Tunisia. *Econ. Geol.* **2013**, *108*, 1425–1457. [[CrossRef](#)]
21. Decrée, S.; Marignac, C.; De Putter, T.; Deloule, E.; Liégeois, J.P.; Demaiffe, D. Pb–Zn mineralization in a Miocene regional extensional context: The case of the Sidi Driss and the Douahria ore deposits (Nefza mining district, northern Tunisia). *Ore Geol. Rev.* **2008**, *34*, 285–303. [[CrossRef](#)]
22. Ben Aissa, R.; Ben Aissa, W.; Ben Haj Amara, A.; Ben Aissa, L.; Tlig, S. The trace and rare earth element contributions to the understanding of Chouichia iron-copper deposits in Northern Tunisia: Metal sources interrelated with magmatism and metamorphism. *Arab. J. Geosci.* **2021**, *14*, 783. [[CrossRef](#)]
23. Jemmali, N.; Souissi, F.; Villa, I.M.; Vennemann, T. Ore genesis of Pb–Zn deposits in the Nappe zone of Northern Tunisia: Constraints from Pb–S–C–O isotopic systems. *Ore Geol. Rev.* **2011**, *40*, 41–53. [[CrossRef](#)]
24. Jemmali, N.; Souissi, F.; Carranza, E.J.M.; Vennemann, T.W. Mineralogical and Geochemical Constraints on the Genesis of the Carbonate-Hosted Jebel Ghozlane Pb–Zn Deposit (Nappe Zone, Northern Tunisia). *Resour. Geol.* **2013**, *63*, 27–41. [[CrossRef](#)]
25. Abidi, R.; Slim-Shimi, N.; Gasquet, D.; Hatira, N.; Somarin, A. Genesis of celestite-bearing cap rock formation from the Ain Allega ore deposit (northern Tunisia): Contributions from microthermometric studies. *Bull. Soc. Géolog. Fr.* **2011**, *182*, 427–435. [[CrossRef](#)]
26. Jemmali, N.; Souissi, F.; Carranza, E.J.M.; Vennemann, T.W.; Bogdanov, K. Geochemical constraints on the genesis of the Pb–Zn deposit of Jalta (northern Tunisia): Implications for timing of mineralization, sources of metals and relationship to the Neogene volcanism. *Geochemistry* **2014**, *74*, 601–613. [[CrossRef](#)]
27. Jemmali, N.; Souissi, F.; Carranza, E.J.M.; Bouabdellah, M. Lead and sulfur isotope constraints on the genesis of the polymetallic mineralization at Oued Maden, Jebel Hallouf and Fedj Hassene carbonate-hosted Pb–Zn (As–Cu–Hg–Sb) deposits, Northern Tunisia. *J. Geochem. Explor.* **2013**, *132*, 6–14. [[CrossRef](#)]
28. Decrée, S.; Marignac, C.; Liégeois, J.P.; Yans, J.; Abdallah, R.B.; Demaiffe, D. Miocene magmatic evolution in the Nefza district (Northern Tunisia) and its relationship with the genesis of polymetallic mineralizations. *Lithos* **2014**, *192*, 240–258. [[CrossRef](#)]

29. Bouillin, J.P. The “Maghreb Basin”; an ancient boundary between Europe and Africa to the west of the Alps. *Bull. Soc. Géolog. Fr.* **1986**, *2*, 547–558. (In French) [[CrossRef](#)]
30. Frizon de Lamotte, D.; Leturmy, P.; Missenard, Y.; Khomsi, S.; Ruiz, G.; Saddiqi, O.; Guillocheau, F.; Michard, A. Mesozoic and Cenozoic vertical movements in the Atlas system (Algeria, Morocco, Tunisia): An overview. *Tectonophysics* **2009**, *475*, 9–28. [[CrossRef](#)]
31. Booth-Rea, G.; Ranero, C.R.; Martínez-Martínez, J.M.; Grevemeyer, I. Crustal types and Tertiary tectonic evolution of the Alborán sea, western Mediterranean. *Geochem. Geophys. Geosyst.* **2007**, *8*, Q10005. [[CrossRef](#)]
32. Durand-Delga, M.; Fontboté, J.M. The structural framework of the Western Mediterranean. In *Colloquium C5: Geology of Alpine chains Derived from the Tethys*; Memoir; Bureau of Geological and Mining Research: Orléans, France, 1980; Volume 11, pp. 65–85. (In French)
33. Van Hinsbergen, D.J.; Vissers, R.L.; Spakman, W. Origin and consequences of western Mediterranean subduction, rollback, and slab segmentation. *Tectonics* **2014**, *33*, 393–419. [[CrossRef](#)]
34. Moragues, L.; Ruano, P.; Azañón, J.M.; Garrido, C.J.; Hidas, K.; Booth Rea, G. Two Cenozoic extensional phases in Mallorca and their bearing on the geodynamic evolution of the western Mediterranean. *Tectonics* **2021**, *40*, e2021TC006868. [[CrossRef](#)]
35. Wildi, W. The Tello-Rifain Chain (Algeria, Morocco, Tunisia): Structure, stratigraphy, and evolution from the Triassic to the Miocene. *Rev. Géogr. Phys. Géolog. Dyn.* **1983**, *24*, 201–297. (In French)
36. Leprière, R.; Frizon de Lamotte, D.; Combier, V.; Gimeno-Vives, O.; Mohn, G.; Eschard, R. The Tell-Rif orogenic system (Morocco, Algeria, Tunisia) and the structural heritage of the southern Tethys margin. *BSGF Earth Sci. Bull.* **2018**, *189*, 10. [[CrossRef](#)]
37. García-Dueñas, V.; Balanyá, J.C.; Martínez-Martínez, J.M. Miocene extensional detachments in the outcropping basement of the northern Alboran basin (Betics) and their tectonic implications. *Geo-Mar. Lett.* **1992**, *12*, 88–95. [[CrossRef](#)]
38. Saadallah, A.; Cabry, R. Alpine extensional detachment tectonics in the Grande Kabylie metamorphic core complex of the Maghrebides (northern Algeria). *Tectonophysics* **1996**, *267*, 257–273. [[CrossRef](#)]
39. Booth-Rea, G.; Jabaloy-Sánchez, A.; Azdimousa, A.; Asebriy, L.; Vílchez, M.V.; Martínez-Martínez, J.M. Upper-crustal extension during oblique collision: The Tamsamani extensional detachment (eastern Rif, Morocco). *Terra Nova* **2012**, *24*, 505–512. [[CrossRef](#)]
40. De la Peña, L.G.; Ranero, C.R.; Gràcia, E.; Booth-Rea, G. The evolution of the westernmost Mediterranean basins. *Earth-Sci. Rev.* **2021**, *214*, 103445. [[CrossRef](#)]
41. Lonergan, L.; White, N. Origin of the Betic-Rif mountain belt. *Tectonics* **1997**, *16*, 504–522. [[CrossRef](#)]
42. Faccenna, C.; Piromallo, C.; Crespo-Blanc, A.; Jolivet, L.; Rossetti, F. Lateral slab deformation and the origin of the western Mediterranean arcs. *Tectonics* **2004**, *23*, TC1012. [[CrossRef](#)]
43. Jolivet, L.; Faccenna, C.; Piromallo, C. From mantle to crust: Stretching the Mediterranean. *Earth Planet. Sci. Lett.* **2009**, *285*, 198–209. [[CrossRef](#)]
44. Teixell, A.; Ayarza, P.; Zeyen, H.; Fernandez, M.; Arboleya, M.L. Effects of mantle upwelling in a compressional setting: The Atlas Mountains of Morocco. *Terra Nova* **2005**, *17*, 456–461. [[CrossRef](#)]
45. Camafort, M.; Pérez-Peña, J.V.; Booth-Rea, G.; Melki, F.; Gràcia, E.; Azañón, J.M.; Galve, J.P.; Marzougui, W.; Gaidi, S.; Ranero, C.R. Active tectonics and drainage evolution in the Tunisian Atlas driven by interaction between crustal shortening and mantle dynamics. *Geomorphology* **2020**, *351*, 106954. [[CrossRef](#)]
46. Faccenna, C.; Becker, T.W. Topographic expressions of mantle dynamics in the Mediterranean. *Earth-Sci. Rev.* **2020**, *209*, 103327. [[CrossRef](#)]
47. Lustrino, M.; Duggen, S.; Rosenberg, C.L. The Central-Western Mediterranean: Anomalous igneous activity in an anomalous collisional tectonic setting. *Earth-Sci. Rev.* **2011**, *104*, 1–40. [[CrossRef](#)]
48. Burrolet, P.F. Structures and tectonics of Tunisia. *Tectonophysics* **1991**, *195*, 359–369. [[CrossRef](#)]
49. Bouaziz, S.; Barrier, E.; Soussi, M.; Turki, M.M.; Zouari, H. Tectonic evolution of the northern African margin in Tunisia from paleostress data and sedimentary record. *Tectonophysics* **2002**, *357*, 227–253. [[CrossRef](#)]
50. Kherroubi, A.; Déverchère, J.; Yelles, A.; De Lépinay, B.M.; Domzig, A.; Cattaneo, A.; Bracène, R.; Gaullier, V.; Graindorge, D. Recent and active deformation pattern off the easternmost Algerian margin, Western Mediterranean Sea: New evidence for contractional tectonic reactivation. *Mar. Geol.* **2009**, *261*, 17–32. [[CrossRef](#)]
51. Melki, F.; Zouaghi, T.; Chelbi, M.B.; Bedir, M.; Zargouni, F. Tectono-sedimentary events and geodynamic evolution of the Mesozoic and Cenozoic basins of the Alpine Margin, Gulf of Tunis, north-eastern Tunisia offshore. *Comptes Rendus Geosci.* **2010**, *342*, 741–753. [[CrossRef](#)]
52. Billi, A.; Faccenna, C.; Bellier, O.; Minelli, L.; Neri, G.; Piromallo, C.; Presti, D.; Scrocca, D.; Serpelloni, E. Recent tectonic reorganization of the Nubia-Eurasia convergent boundary heading for the closure of the western Mediterranean. *Bull. Soc. Géolog. Fr.* **2011**, *182*, 279–303. [[CrossRef](#)]
53. Giaconia, F.; Booth-Rea, G.; Ranero, C.R.; Gràcia, E.; Bartolome, R.; Calahorrano, A.; Lo Iacono, C.; Vendrell, M.G.; Cameselle, A.L.; Costa, S.; et al. Compressional tectonic inversion of the Algero-Balearic basin: Latest Miocene to present oblique convergence at the Palomares margin (Western Mediterranean). *Tectonics* **2015**, *34*, 1516–1543. [[CrossRef](#)]

54. Zitellini, N.; Ranero, C.R.; Loreto, M.F.; Ligi, M.; Pastore, M.; D’Oriano, F.; Sallares, V.; Grevemeyer, I.; Moeller, S.; Prada, M. Recent inversion of the Tyrrhenian Basin. *Geology* **2020**, *48*, 123–127. [[CrossRef](#)]
55. De la Peña, L.; Ranero, C.R.; Gràcia, E.; Booth-Rea, G.; Azañón, J.M.; Tinivella, U.; Yelles-Chaouche, A. Evidence for a developing plate boundary in the western Mediterranean. *Nat. Commun.* **2022**, *13*, 4786. [[CrossRef](#)]
56. Favre, P.; Stampfli, G.; Wildi, W. Jurassic sedimentary record and tectonic evolution of the northwestern corner of Africa. *Palaeogeogr. Palaeoclimatol. Palaeoecol.* **1991**, *87*, 53–73. [[CrossRef](#)]
57. Dewey, J.F.; Helman, M.L.; Knott, S.D.; Turco, E.; Hutton, D.H.W. Kinematics of the western Mediterranean. *Geol. Soc. Lond. Spec. Publ.* **1989**, *45*, 265–283. [[CrossRef](#)]
58. Rosenbaum, G.; Lister, G.S.; Duboz, C. Relative motions of Africa, Iberia and Europe during Alpine orogeny. *Tectonophysics* **2002**, *359*, 117–129. [[CrossRef](#)]
59. Boukaoud, E.H.; Godard, G.; Chabou, M.C.; Bouftouha, Y.; Doukkari, S. Petrology and geochemistry of the Texenna ophiolites, northeastern Algeria: Implications for the Maghrebien flysch suture zone. *Lithos* **2021**, *390*, 106019. [[CrossRef](#)]
60. Caby, R.; Bruguier, O.; Fernandez, L.; Hammor, D.; Bosch, D.; Mechat, M.; Laouar, R.; Ouabadi, A.; Abdallah, N.; Douchet, C. Metamorphic diamonds in a garnet megacryst from the Edough Massif (northeastern Algeria). Recognition and geodynamic consequences. *Tectonophysics* **2014**, *637*, 341–353. [[CrossRef](#)]
61. Bruguier, O.; Bosch, D.; Caby, R.; Vitale-Brovarone, A.; Fernandez, L.; Hammor, D.; Laouar, L.; Ouabadi, A.; Abdallah, N.; Mechat, M. Age of UHP metamorphism in the Western Mediterranean: Insight from rutile and minute zircon inclusions in a diamond-bearing garnet megacryst (Edough Massif, NE Algeria). *Earth Planet. Sci. Lett.* **2017**, *474*, 215–225. [[CrossRef](#)]
62. Marrone, S.; Monié, P.; Rossetti, F.; Lucci, F.; Theye, T.; Bouybaouene, M.L.; Zaghoul, M.N. The pressure–temperature–time–deformation history of the Beni Mzala unit (Upper Sebides, Rif belt, Morocco): Refining the Alpine tectono-metamorphic evolution of the Alboran Domain of the western Mediterranean. *J. Metamorph. Geol.* **2021**, *39*, 591–615. [[CrossRef](#)]
63. Bessière, E.; Scaillet, S.; Augier, R.; Jolivet, L.; Miguel Azañón, J.; Booth-Rea, G.; Romagny, A.; Duval, F. 40Ar/39Ar age constraints on HP/LT metamorphism in extensively overprinted units: The example of the Alpujarride subduction complex (Betic Cordillera, Spain). *Tectonics* **2022**, *41*, e2021TC006889. [[CrossRef](#)]
64. Platt, J.P.; Whitehouse, M.J.; Kelley, S.P.; Carter, A.; Hollick, L. Simultaneous extensional exhumation across the Alboran Basin: Implications for the causes of late orogenic extension. *Geology* **2003**, *31*, 251–254. [[CrossRef](#)]
65. Garrido, C.J.; Gueydan, F.; Booth-Rea, G.; Precigout, J.; Hidas, K.; Padrón-Navarta, J.A.; Marchesi, C. Garnet lherzolite and garnet-spinel mylonite in the Ronda peridotite: Vestiges of Oligocene backarc mantle lithospheric extension in the western Mediterranean. *Geology* **2011**, *39*, 927–930. [[CrossRef](#)]
66. Marchesi, C.; Garrido, C.J.; Bosch, D.; Bodinier, J.L.; Hidas, K.; Padron-Navarta, J.A.; Gervilla, F. A Late Oligocene suprasubduction setting in the westernmost Mediterranean revealed by intrusive pyroxenite dikes in the Ronda peridotite (southern Spain). *J. Geol.* **2012**, *120*, 237–247. [[CrossRef](#)]
67. Belayouni, H.; Guerrero, F.; Martín-Martín, M.; Serrano, F. Paleogeographic and geodynamic Miocene evolution of the Tunisian Tell (Numidian and Post-Numidian successions): Bearing with the Maghrebien chain. *Int. J. Earth Sci.* **2013**, *102*, 831–855. [[CrossRef](#)]
68. Bellon, H.; Perthuisot, V. Radiometric ages (K/Ar) of potassic feldspars and neofomed micas in the Triassic of Northern Tunisia. *Bull. Soc. Géolog. Fr.* **1977**, *7*, 1179–1184. (In French) [[CrossRef](#)]
69. Jallouli, C.; Mickus, K.; Turki, M.M.; Rihane, C. Gravity and aeromagnetic constraints on the extent of Cenozoic volcanic rocks within the Nefza–Tabarka region, northwestern Tunisia. *J. Volcanol. Geotherm. Res.* **2003**, *122*, 51–68. [[CrossRef](#)]
70. Riahi, S.; Soussi, M.; Stow, D. Sedimentological and stratigraphic constraints on Oligo–Miocene deposition in the Mogod Mountains, northern Tunisia: New insights for paleogeographic evolution of North Africa passive margin. *Int. J. Earth Sci.* **2021**, *110*, 653–688. [[CrossRef](#)]
71. Ben Ferjani, F.; Burrolet, P.F.; Mejri, F. *Petroleum Geology of Tunisia*; Entreprise Tunisienne des Activités Pétrolières (ETAP): Irvine, CA, USA, 1990; 194p.
72. Ben Haj Ali, M.; Jedoui, Y.; Dali, T.; Ben Salem, H.; Memmi, L. *Geological Map of Tunisia, Scale 1/500.000*; Office National des Mines, Service Géologique: Tunis, Tunisia, 1985. (In French)
73. Naji, C.; Masrouhi, A.; Amri, Z.; Gharbi, M.; Bellier, O. Cretaceous paleomargin tilted blocks geometry in northern Tunisia: Stratigraphic consideration and fault kinematic analysis. *Arab. J. Geosci.* **2018**, *11*, 583. [[CrossRef](#)]
74. Troudi, H.; Tari, G.; Alouani, W.; Cantarella, G. Styles of salt tectonics in Central Tunisia: An overview. In *Permo-Triassic Salt Provinces of Europe, North Africa and the Atlantic Margins*; Elsevier: Amsterdam, The Netherlands, 2017; pp. 543–561.
75. Caby, R.; Hammor, D.; Delor, C. Metamorphic evolution, partial melting and Miocene exhumation of lower crust in the Edough metamorphic core complex, west Mediterranean orogen, eastern Algeria. *Tectonophysics* **2001**, *342*, 239–273. [[CrossRef](#)]
76. Belayouni, H.; Brunelli, D.; Clocchiatti, R.; Di Staso, A.; El Hassani, I.E.E.A.; Guerrero, F.; Kassaa, S.; Laridhi-Ouazaa, N.; Martín, M.M.; Serrano, F.; et al. La Galite Archipelago (Tunisia, North Africa): Stratigraphic and petrographic revision and insights for geodynamic evolution of the Maghrebien Chain. *J. Afr. Earth Sci.* **2010**, *56*, 15–28. [[CrossRef](#)]

77. Marignac, C.; Aïssa, D.E.; Cheilletz, A.; Gasquet, D. Edough-Cap de Fer Polymetallic District, Northeast Algeria: II. Metallogenic Evolution of a Late Miocene Metamorphic Core Complex in the Alpine Maghrebide Belt. In *Mineral Deposits of North Africa; Mineral Resource Reviews, Series*; Bouabdellah, M., Slack, J.F., Eds.; Springer International Publishing: Cham, Switzerland, 2016; pp. 167–200. ISBN 978-3-319-31731-1/. [[CrossRef](#)]
78. Melki, F.; Zouaghi, T.; Harrab, S.; Sainz, A.C.; Bédir, M.; Zargouni, F. Structuring and evolution of Neogene transcurrent basins in the Tellian foreland domain, north-eastern Tunisia. *J. Geodyn.* **2011**, *52*, 57–69. [[CrossRef](#)]
79. Rouvier, H. Geology of extreme Northern Tunisia: Superimposed tectonics and paleogeographies at the Eastern end of the North-Maghrebine chain. *Ann. Mines Geol.* **1985**, *29*, 427. (In French)
80. Melki, F.; Zouaghi, T.; Ben Chelbi, M.; Bédir, M.; Zargouni, F. Role of the NE-SW Hercynian master fault systems and associated lineaments on the structuring and evolution of the Mesozoic and Cenozoic basins of the Alpine Margin, northern Tunisia. In *Tectonics: Recent Advances*; BoD—Books on Demand: Norderstedt, Germany, 2012; pp. 131–168.
81. Essid, E.M.; Kadri, A.; Inoubli, M.H.; Zargouni, F. Identification of new NE-trending deep-seated faults and tectonic pattern updating in northern Tunisia (Mogodos–Bizerte region), insights from field and seismic reflection data. *Tectonophysics* **2016**, *682*, 249–263. [[CrossRef](#)]
82. Essid, E.M.; Kadri, A.; Balti, H.; Gasmi, M.; Zargouni, F. Contributions of gravity and field data on the structural scheme updating of the Tellian domain and its foreland (Nefza-Bizerte region, northern Tunisia). *Int. J. Earth Sci.* **2018**, *107*, 2357–2381. [[CrossRef](#)]
83. Gaidi, S.; Galve, J.P.; Melki, F.; Ruano, P.; Reyes-Carmona, C.; Marzougui, W.; Devoto, S.; Pérez-Peña, J.V.; Azañón, J.M.; Chouaieb, H.; et al. Analysis of the geological controls and kinematics of the chgega landslide (Mateur, Tunisia) exploiting photogrammetry and InSAR technologies. *Remote Sens.* **2021**, *13*, 4048. [[CrossRef](#)]
84. Bejaoui, H.; Aifa, T.; Melki, F.; Zargouni, F. Structural evolution of Cenozoic basins in northeastern Tunisia, in response to sinistral strike-slip movement on the El Alia-Teboursouk Fault. *J. Afr. Earth Sci.* **2017**, *134*, 174–197. [[CrossRef](#)]
85. Gaidi, S.; Booth-Rea, G.; Melki, F.; Marzougui, W.; Ruano, P.; Pérez-Peña, J.V.; Azañón, J.M.; Zargouni, F.; Chouaieb, H.; Galve, J.P. Active fault segmentation in Northern Tunisia. *J. Struct. Geol.* **2020**, *139*, 104146. [[CrossRef](#)]
86. Gharbi, M. Study of Mercury Mineralizations of the Ghardimaou-Cap Serrat Fault (Northwestern Tunisia). Master's Thesis, Ecole Nationale Supérieure Géologie, Nancy, France, 1977; 131p. (In French)
87. Rouvier, H. Geology of Extreme Northern Tunisia: Superimposed Tectonics and Paleogeographies at the Eastern End of the North-Maghrebine Chain. Ph.D. Thesis, Université de Paris VI, Paris, France, 1977; 898p. (In French)
88. Talbi, F.; Melki, F.; Ismail-Lattrache, K.B.; Alouani, R.; Tlig, S. The Numidian of Northern Tunisia: Stratigraphic data and geodynamic Interpretation. *Estud. Geológ.* **2008**, *64*, 31–44. (In French) [[CrossRef](#)]
89. Frizon de Lamotte, D.; Saint Bezar, B.; Bracène, R.; Mercier, E. The two main steps of the Atlas building and geodynamics of the western Mediterranean. *Tectonics* **2000**, *19*, 740–761. [[CrossRef](#)]
90. Khomsi, S.; Soussi, M.; Mahersi, C.; Bédir, M.; Jemia, H.F.B.; Riahi, S.; Khalfa, K.B. New insights on the structural style of the subsurface of the Tell units in north-western Tunisia issued from seismic imaging: Geodynamic implications. *Comptes Rendus Geosci.* **2009**, *341*, 347–356. [[CrossRef](#)]
91. Bellon, N. Neogene and Quaternary Magmatic Series of the Western Mediterranean Basin Compared Within Their Geodynamic Framework: Geodynamic Implications. Ph.D. Thesis, Université Paris-Sud, Orsay, France, 1976; 363p. (In French)
92. Halloul, N.; Gourgau, A. The post-collisional volcanism of northern Tunisia: Petrology and evolution through time. *J. Afr. Earth Sci.* **2012**, *63*, 62–76. [[CrossRef](#)]
93. Yans, J.; Verhaert, M.; Gautheron, C.; Antoine, P.O.; Moussi, B.; Dekoninck, A.; Decrée, S.; Chaftar, H.R.; Hatira, N.; Dupuis, C.; et al. (U-Th)/He Dating of Supergene Iron (Oxyhydr-) Oxides of the Nefza-Sejnane District (Tunisia): New Insights into Mineralization and Mammalian Biostratigraphy. *Minerals* **2021**, *11*, 260. [[CrossRef](#)]
94. Fichtner, A.; Villaseñor, A. Crust and upper mantle of the western Mediterranean—Constraints from full-waveform inversion. *Earth Planet. Sci. Lett.* **2015**, *428*, 52–62. [[CrossRef](#)]
95. Aichaoui, M.; Abtout, A.; Bourouis, S.; Bouyahiaoui, B. Crustal and upper mantle structure of northern Algeria inferred from a 3-D inversion of teleseismic tomography. *J. Afr. Earth Sci.* **2022**, *190*, 104501. [[CrossRef](#)]
96. Lamiri, S.; Radi, Z.; Layadi, K. Geodynamic evolution of north-east Algerian basin: 3D velocity model Reveals high-temperature flow. *J. Afr. Earth Sci.* **2024**, *209*, 105122. [[CrossRef](#)]
97. Research Group for Lithospheric Structure in Tunisia. The EGT'85 seismic experiment in Tunisia: A reconnaissance of the deep structures. *Tectonophysics* **1992**, *207*, 245–267. [[CrossRef](#)]
98. Bahrouni, N.; Masson, F.; Meghraoui, M.; Saleh, M.; Maamri, R.; Dhaha, F.; Arfaoui, M. Active tectonics and GPS data analysis of the Maghrebian thrust belt and Africa-Eurasia plate convergence in Tunisia. *Tectonophysics* **2020**, *785*, 228440. [[CrossRef](#)]
99. Soumaya, A.; Kadri, A.; Ayed, N.B.; Kim, Y.S.; Dooley, T.P.; Rajabi, M.; Braham, A. Deformation styles related to intraplate strike-slip fault systems of the Saharan-Tunisian Southern Atlas (North Africa): New kinematic models. *J. Struct. Geol.* **2020**, *140*, 104175. [[CrossRef](#)]

100. Mansouri, A. Pb-Zn Deposits and Karstification in a Continental Environment: The Jbel Hallouf-Sidi Bou Aouane District (Northern Tunisia). Ph.D. Thesis, University de Pierre et Marie Curie, Paris, France, 1980; 199p. (In French)
101. Slim-Shimi, N. Mineralogy and Paragenesis of Polymetallic Deposits in the Nappes Zone of Tunisia. Geochemical Conditions of Deposition and Genetic Implications. Ph.D. Thesis, Faculté des Sciences De Tunis, Tunis, Tunisia, 1992; 268p. (In French)
102. Slim-Shimi, N.; Tlig, S. Mixed type sulfide deposits in Northern Tunisia, regenerated in relation to paleogeography and tectonism. *J. Afr. Earth Sci.* **1993**, *16*, 287–307. [[CrossRef](#)]
103. Decrée, S.; Marignac, C.; Abidi, R.; Jemmali, N.; Deloule, E.; Souissi, F. Tectonomagmatic context of SEDEX Pb–Zn and polymetallic Ore deposits of the Nappe zone Northern Tunisia, and comparisons with MVT deposits in the region. In *Mineral Deposits of North Africa*; Springer: Cham, Switzerland, 2016; pp. 497–525.
104. Abidi, R.; Marignac, C.; Deloule, E.; Hibsich, C.; Gasquet, D.; Renac, C.; Somarin, A.K.; Hatira, N.; Slim-Shimi, N. Interplay of magmatic and diapiric environments in the Djebel El Hamra Pb–Zn–Hg ore district, northern Tunisia. *Miner. Depos.* **2022**, *57*, 35–60. [[CrossRef](#)]
105. Savelli, C. Time–space distribution of magmatic activity in the western Mediterranean and peripheral orogens during the past 30 Ma (a stimulus to geodynamic considerations). *J. Geodyn.* **2002**, *34*, 99–126. [[CrossRef](#)]
106. Talbi, F.; Jaafari, M.; Tlig, S. Neogene magmatism of Northern Tunisia: Petrogenesis and geodynamic events. *Rev. Soc. Geológica Esp.* **2005**, *18*, 241–252. (In French)
107. Faccenna, C.; Becker, T.W.; Auer, L.; Billi, A.; Boschi, L.; Brun, J.P.; Capitanio, F.A.; Funiciello, F.; Horvath, F.; Jolivet, L.; et al. Mantle dynamics in the Mediterranean. *Rev. Geophys.* **2014**, *52*, 283–332. [[CrossRef](#)]
108. Van der Meer, D.G.; Van Hinsbergen, D.J.; Spakman, W. Atlas of the underworld: Slab remnants in the mantle, their sinking history, and a new outlook on lower mantle viscosity. *Tectonophysics* **2018**, *723*, 309–448. [[CrossRef](#)]
109. Soumaya, A.; Ben Ayed, N.; Delvaux, D.; Ghanmi, M. Spatial variation of present-day stress field and tectonic regime in Tunisia and surroundings from formal inversion of focal mechanisms: Geodynamic implications for central Mediterranean. *Tectonics* **2015**, *34*, 1154–1180. [[CrossRef](#)]
110. Crampon, N. Geological Study of the Mogods Border, the Bizerte Region, and the North of Hedil (Northern Tunisia). Ph.D. Thesis, Université de Nancy I, Nancy, France, 1971; 522p. (In French)
111. Laridhi-Ouazaa, N. Evidence of a mineralogical and geochemical identity between the rhyodacite of Ain Deflaia and the pyroclastics of the Oued Zouaraa sedimentary Basin (Nefza: Northern Tunisia). *Comptes Rendus Académie Sci.* **1989**, *309*, 1571–1576. (In French)
112. Mauduit, F. The Neogene Volcanism of Continental Tunisia. Ph.D. Thesis, Université Paris, Paris, France, 1978; 158p. (In French)
113. Rekhiss, F. The Galite Archipelago, a landmark between the Kabyle massifs and the Peloritani mountains (Western Mediterranean, Northern Tunisian margin). *Géolog. Méditerran.* **1996**, *23*, 201–210. (In French) [[CrossRef](#)]
114. Maury, R.C.; Fourcade, S.; Coulon, C.; Bellon, H.; Coutelle, A.; Ouabadi, A.; Semroud, B.; Megartsi, M.; Cotten, J.; Belanteur, O.; et al. Post-collisional Neogene magmatism of the Mediterranean Maghreb margin: A consequence of slab breakoff. *Comptes Rendus L'acad. Sci. Ser. IIA Earth Planet. Sci.* **2000**, *331*, 159–173.
115. Jemmali, N. Contributions of Trace Element Geochemistry, Isotopic Geochemistry (C, O, S, Pb), and Fluid Inclusions to the Study of Mineral Deposits in Northern Tunisia: Origin of Metals, Age of Mineralizations, and Genetic Model. Habilitation Thesis, Faculty of Sciences of Tunis, Tunis, Tunisia, 2023; 145p. (In French)
116. Albidon Limited. Exploration Report. 2004. Available online: <https://ww38.albidon.com/documents/Nefza2.pdf> (accessed on 1 November 2013).
117. Slim-Shimi, N.; Moëlo, Y.; Tlig, S.; Levy, C. Sulfide geochemistry and genesis of Chouichia and Ain el Bey copper deposits in northwestern Tunisia. *Miner. Depos.* **1996**, *31*, 188–200. [[CrossRef](#)]
118. Sainfeld, P. The lead-zinc-bearing deposits of Tunisia. *Econ. Geol.* **1956**, *51*, 150–177. [[CrossRef](#)]
119. Rekhiss, F. Structural Model and Geodynamic Evolution at the Eastern End of the North African Alpine Chain. Ph.D Thesis, El-Manar University, Tunis, Tunisia, 2007; 285p. (In French)
120. Talbi, F. Petrology, Geochemistry, Study of Fluid Phases, and Mineralization Related to Neogene Magmatism in Northern Tunisia. Ph.D. Thesis, Université de Tunis II, Tunis, Tunisia, 1998; 368p. (In French)
121. Sainfeld, P. The Lead-Zinc deposits of Tunisia. *Ann. Min. Géol. Tunis* **1952**, *9*, 1–285. (In French)
122. Jaafari, M. Geodynamics, Basic Magmatism, and Mineralizations of the Mogods: Petrology, Geochemistry, and Fluid Inclusions. Ph.D. Thesis, Faculté des Sciences de Tunis, Tunis, Tunisia, 1997; 343p. (In French)
123. Slim, N. Mineralogical Study of Copper and Lead-Zinc Deposits in Northern Tunisia. Ph.D. Thesis, University Paris VI, Paris, France, 1981; 240p. (In French)
124. Zhu, B.Q. *Theory and Application of Isotopic Systematic in Earth Science*; Science Press: Beijing, China, 1998; 330p.
125. Juteau, M.; Michard, A.; Albarede, F. The Pb–Sr–Nd isotope geochemistry of some recent circum-Mediterranean granites. *Contrib. Mineral. Petrol.* **1986**, *92*, 331–340. [[CrossRef](#)]

126. Duggen, S.; Hoernle, K.; Van den Bogaard, P.; Harris, C. Magmatic evolution of the Alboran region: The role of subduction in forming the western Mediterranean and causing the Messinian Salinity Crisis. *Earth Planet. Sci. Lett.* **2004**, *218*, 91–108. [[CrossRef](#)]
127. Zartman, R.E.; Doe, B.R. Plumbotectonics—The model. *Tectonophysics* **1981**, *75*, 135–162. [[CrossRef](#)]
128. Zartman, R.E.; Haines, S.M. The plumbotectonic model for Pb isotopic systematics among major terrestrial reservoirs—A case for bi-directional transport. *Geochim. Cosmochim. Acta* **1988**, *52*, 1327–1339. [[CrossRef](#)]
129. Evans, A.M. *An Introduction to Economic Geology and Its Environmental Impact*; Wiley-Blackwell: Hoboken, NJ, USA, 1997; 376p.
130. Touahri, B. Geochemistry and Metallogeny of Lead and Zinc Mineralizations in Northern Algeria. Ph.D. Thesis, Université Pierre Marie Curie (Paris 6), Paris, France, 1987; 380p. (In French)
131. Lebret, N. Structural and Metallogenic Context of Magnetite Skarns in Beni Bou Ifrouer (Eastern Rif, Morocco): Contributions to the Geodynamic Evolution of the Western Mediterranean. Ph.D. Thesis, Université Orléans, Orleans, France, 2014; 477p. (In French)
132. Arribas, A.; Tosdal, R.M. Isotopic composition of Pb in ore deposits of the Betic Cordillera, Spain; origin and relationship to other European deposits. *Econ. Geol.* **1994**, *89*, 1074–1093. [[CrossRef](#)]
133. Albarède, F.; Desaulty, A.M.; Blichert-Toft, J. A geological perspective on the use of Pb isotopes in archaeometry. *Archaeometry* **2012**, *54*, 853–867. [[CrossRef](#)]
134. Stacey, J.S.; Kramers, J.D. Approximation of terrestrial lead isotope evolution by a two-stage model. *Earth Planet. Sci. Lett.* **1975**, *26*, 207–221. [[CrossRef](#)]
135. Chiaradia, M.; Fontboté, L.; Paladines, A. Metal sources in mineral deposits and crustal rocks of Ecuador (1 N–4 S): A lead isotope synthesis. *Econ. Geol.* **2004**, *99*, 1085–1106.
136. Huston, D.L.; Champion, D.C.; Cassidy, K.F. Tectonic controls on the endowment of Neoproterozoic cratons in volcanic-hosted massive sulfide deposits: Evidence from lead and neodymium isotopes. *Econ. Geol.* **2014**, *109*, 11–26. [[CrossRef](#)]
137. Badgasarian, G.P.; Bajanik, S.; Vass, D. Radiometric age of Neogene volcanism in Northern Tunisia. *Notes Serv. Géolog. Tunis.* **1972**, *40*, 79–85. (In French)
138. Doe, B.R. Common Lead. In *Lead Isotopes*; Springer: Berlin/Heidelberg, Germany, 1970; pp. 35–78.
139. Faure, G.; Mensing, T.M. *Principles and Applications*; John Wiley & Sons, Inc.: Hoboken, NJ, USA, 2005; p. 897.
140. Haidar, S.; Déverchère, J.; Graindorge, D.; Arab, M.; Medaouri, M.; Klingelhoefer, F. Back-arc dynamics controlled by slab rollback and tearing: A reappraisal of seafloor spreading and kinematic evolution of the Eastern Algero-Balearic basin (western Mediterranean) in the Middle-Late Miocene. *Tectonics* **2022**, *41*, e2021TC006877. [[CrossRef](#)]
141. Duggen, S.; Hoernle, K.; Klügel, A.; Geldmacher, J.; Thirlwall, M.; Hauff, F.; Lowry, D.; Oates, N. Geochemical zonation of the Miocene Alborán Basin volcanism (westernmost Mediterranean): Geodynamic implications. *Contrib. Mineral. Petrol.* **2008**, *156*, 577–593. [[CrossRef](#)]
142. Booth-Rea, G.; Ranero, C.R.; Grevemeyer, I. The Alboran volcanic-arc modulated the Messinian faunal exchange and salinity crisis. *Sci. Rep.* **2018**, *8*, 13015. [[CrossRef](#)]
143. Zeck, H.P.; Williams, I.S. Inherited and Magmatic Zircon from Neogene Hoyazo Cordierite Dacite, SE Spain—Anatectic Source Rock Provenance and Magmatic Evolution: In Memoriam Professor Chris Powell. *J. Petrol.* **2002**, *43*, 1089–1104. [[CrossRef](#)]
144. Arribas, A.; Cunningham, C.G.; Rytuba, J.J.; Rye, R.O.; Kelly, W.C.; Podwysocki, M.H.; McKee, E.H.; Tosdal, R.M. Geology, geochronology, fluid inclusions, and isotope geochemistry of the Rodalquilar gold alunite deposit, Spain. *Econ. Geol.* **1995**, *90*, 795–822. [[CrossRef](#)]
145. Martínez-Frías, J. An ancient Ba-Sb-Ag-Fe-Hg-bearing hydrothermal system in SE Spain. *Epis. J. Int. Geosci.* **1998**, *21*, 248–251. [[CrossRef](#)] [[PubMed](#)]
146. Dyja, V.; Hibsich, C.; Tarantola, A.; Cathelineau, M.; Boiron, M.C.; Maignac, C.; Bartier, D.; Carrillo-Rosúa, J.; Morales Ruano, S.; Boulvais, P. From deep to shallow fluid reservoirs: Evolution of fluid sources during exhumation of the Sierra Almagrera, Betic Cordillera, Spain. *Geofluids* **2016**, *16*, 103–128. [[CrossRef](#)]
147. Reynolds, N.A.; Large, D. Tethyan zinc-lead metallogeny in Europe, North Africa, and Asia. In *The Challenge of Finding New Mineral Resources: Global Metallogeny, Innovative Exploration, and New Discoveries*; Society of Economic Geologists: Littleton, CO, USA, 2010; Volume 15, pp. 339–365.
148. Blundell, D.J. The timing and location of major ore deposits in an evolving orogen: The geodynamic context. *Geol. Soc. Lond. Spec. Publ.* **2002**, *204*, 1–12. [[CrossRef](#)]
149. Lips, A.L. Correlating magmatic-hydrothermal ore deposit formation over time with geodynamic processes in SE Europe. *Geol. Soc. Lond. Spec. Publ.* **2002**, *204*, 69–79. [[CrossRef](#)]

Disclaimer/Publisher’s Note: The statements, opinions and data contained in all publications are solely those of the individual author(s) and contributor(s) and not of MDPI and/or the editor(s). MDPI and/or the editor(s) disclaim responsibility for any injury to people or property resulting from any ideas, methods, instructions or products referred to in the content.